A&A 616, A149 (2018)
https://doi.org/10.1051/0004-6361/201832787

Astronomy & Astrophysics

Search for Galactic runaway stars using *Gaia* Data Release 1 and HIPPARCOS proper motions⋆

J. Maíz Apellániz[1], M. Pantaleoni González[1,2], R. H. Barbá[3], S. Simón-Díaz[4,5], I. Negueruela[6], D. J. Lennon[7], A. Sota[8], and E. Trigueros Páez[1,6]

[1] Centro de Astrobiología, CSIC-INTA, Campus ESAC, Camino Bajo del Castillo s/n, 28 692 Villanueva de la Cañada, Spain
e-mail: jmaiz@cab.inta-csic.es
[2] Departamento de Astrofísica y Física de la Atmósfera, Universidad Complutense de Madrid, 28 040 Madrid, Spain
[3] Departamento de Física y Astronomía, Universidad de La Serena, Av. Cisternas 1200 Norte, La Serena, Chile
[4] Instituto de Astrofísica de Canarias, 38 200 La Laguna, Tenerife, Spain
[5] Departamento de Astrofísica, Universidad de La Laguna, 38 205 La Laguna, Tenerife, Spain
[6] Departamento de Física, Ingeniería de Sistemas y Teoría de la Señal, Escuela Politécnica Superior, Universidad de Alicante, Carretera San Vicente del Raspeig s/n, 03 690 San Vicente del Raspeig, Spain
[7] ESA - European Space Astronomy Centre, Camino Bajo del Castillo s/n, 28 692 Villanueva de la Cañada, Spain
[8] Instituto de Astrofísica de Andalucía-CSIC Glorieta de la Astronomía s/n, 18 008 Granada, Spain

Received 7 February 2018 / Accepted 20 April 2018

ABSTRACT

Context. The first *Gaia* Data Release (DR1) significantly improved the previously available proper motions for the majority of the *Tycho*-2 stars.
Aims. We wish to detect runaway stars using *Gaia* DR1 proper motions and compare our results with previous searches.
Methods. Runaway O stars and BA supergiants were detected using a 2D proper motion method. The sample was selected using Simbad, spectra from our GOSSS project, literature spectral types, and photometry processed using the code CHORIZOS.
Results. We detect 76 runaway stars, 17 (possibly 19) of them with no prior identification as such, with an estimated detection rate of approximately one half of the real runaway fraction. An age effect appears to be present, with objects of spectral subtype B1 and later having traveled for longer distances than runaways of earlier subtypes. We also tentatively propose that the fraction of runaways is lower among BA supergiants that among O stars, but further studies using future *Gaia* data releases are needed to confirm this. The frequency of fast rotators is high among runaway O stars, which indicates that a significant fraction of them (and possibly the majority) is produced in supernova explosions.

Key words. surveys – proper motions – Galaxy: structure – supergiants – stars: kinematics and dynamics – stars: early-type

1. Introduction

Runaway stars are (usually massive) Population I stars that move at high peculiar velocities with respect to the mean Galactic rotation. Two mechanisms were proposed more than half a century ago to explain their production: the ejection of a close companion in a supernova explosion (Blaauw 1961), and a three- or more-body interaction at the core of a compact stellar cluster (Poveda et al. 1967). Runaway stars can be detected by their proper motions, radial velocities, or through a combination of both. The availability of good-quality proper motions from HIPPARCOS allowed many new runaway stars to be detected (Hoogerwerf et al. 2001; Mdzinarishvili 2004; Mdzinarishvili & Chargeishvili 2005; Tetzlaff et al. 2011).

The success in the detection of runaway stars with HIPPARCOS led to great expectations for *Gaia*. On 14 September 2016, the first *Gaia* Data Release (DR1) was presented (Brown et al. 2016). *Gaia* DR1 includes parallaxes and proper motions from the *Tycho-Gaia* astrometric solution (TGAS; Michalik et al. 2015) for the majority (but not all) of the *Tycho*-2 stars. Among the excluded *Tycho*-2 stars, we find all of the very bright objects, but also some dimmer stars. TGAS proper motions exist for a significantly larger number of stars than for HIPPARCOS, and for the stars in common between both catalogs, they are more precise.

Good-quality proper motions and/or radial velocities are a requirement to detect runaway stars, though other characteristics such as the presence of a bow shock can also provide indications of their nature. We also need to correctly identify a sample of massive stars to detect runaway stars because these objects are like a needle in a haystack of hot evolved low-mass stars where the range of proper motions and radial velocities can be large because of their relative proximity and the mixture of populations. The Galactic O-Star Spectroscopic Survey (GOSSS, Maíz Apellániz et al. 2011) can play a fundamental helping role here. GOSSS is obtaining $R \sim 2500$ blue-violet spectroscopy with a high signal-to-noise ratio (S/N) of all optically accessible Galactic O stars. To this date, three survey papers (Sota et al. 2011, 2014; Maíz Apellániz et al. 2016) have

⋆ The spectral types in Table 2 will be added to the spectral types in the three GOSSS survey papers and in Maíz Apellániz et al. (2018) and the resulting table will be available from the GOSC web site http://gosc.cab.inta-csic.es.

been published with a total of 590 O stars[1]. An additional several hundreds of O stars and several thousands of B- and later-type stars have been observed, and their data will be published in the near future. One reason why GOSSS is needed is given by Maíz Apellániz et al. (2013): at the time when this paper was published, 24.9% of the O stars with previous spectral classifications that GOSSS had observed were found to be of other spectral type (some were even late-type stars; Maíz Apellániz et al. 2016). Five years later, the number of such false positives in GOSSS is ~35%. Therefore, finding an object with a peculiar proper motion that according to the Simbad database is an O star could be a new runaway star or it could be something else: some confirmation such as a good spectrogram is needed before one can be certain.

A preliminary version of the results in this paper was presented in Maíz Apellániz et al. (2017b), from now on Paper I. This contribution was limited to O stars. Here we include additional O stars in our sample, extend it to BA supergiants, present new spectra and information, and discuss our procedures and results in more detail, as Paper I was a relatively brief non-refereed contribution to conference proceedings.

2. Data and methods

The core data of this paper are the *Gaia* DR1 and HIPPARCOS proper motions for Galactic massive stars presented in the next subsection. We also used supporting data in the form of spectra, photometry, and images, which are presented in the following subsections.

2.1. Proper motions

When *Gaia* DR1 was announced, our initial plan was to analyze the included TGAS parallaxes to increase the small number of useful trigonometric distances available for O stars (van Leeuwen 2007; Maíz Apellániz et al. 2008). However, the TGAS parallaxes for O stars provide little new information, as the brightest O stars are not included, and only one star, AE Aur, has $\pi_o/\sigma_\pi > 6$, where π_o is the observed parallax and σ_π is the parallax uncertainty. We recall that in general, $\langle d \rangle > \neq 1/\pi_o$, that is, the inverse of the observed parallax is not an unbiased estimator of the trigonometric distance (Lutz & Kelker 1973; Maíz Apellániz 2001, 2005).

On the other hand, the TGAS proper motions proved to have useful information. We used three different samples:

1. O stars that had been observed with GOSSS when this work started. This was the sample in Paper I.
2. Additional objects for which an O-type classification appeared in Simbad.
3. Objects classified as BA supergiants in Simbad.

The first sample is a "clean" sample: uniformly selected, with a coherent magnitude limit over the whole sky (complete to $B = 8$ and near-complete to $B = 10$), and with few expected false positives[2]. The situation is different for the other two samples, which are more mixed. Therefore, after cross-matching them with entries with TGAS and/or HIPPARCOS proper motions, we had to clean them, as explained below.

Table 1. Samples used in this paper.

Sample	Sp. ty.	T	H	T or H	R	R%	D
1+2	O	770	325	871	48[a]	5.7	26
3	BA I	833	427	959	27	3.1	79

Notes. T and H refer to TGAS and HIPPARCOS, respectively, and the columns indicate the number of entries in these catalogs. R is the number of runaway candidates, R% is the percentage of runaways, and D is the number of discarded objects. [(a)]Not including ALS 18 929, see below.

We cross-matched each of the samples with the TGAS and HIPPARCOS (van Leeuwen 2007) catalogs. The numbers of objects found are given in Table 1. We note that since some objects have both TGAS and HIPPARCOS proper motions, the third number in each row is always smaller than the sum of the other two (bright objects are generally absent from TGAS and dim objects from HIPPARCOS). When an object had entries in both catalogs, we chose TGAS. We initially cleaned all samples by excluding all cases where the uncertainties in the proper motions were too large to be useful to determine the runaway character of the object. We additionally cleaned the last two samples for stars for which the analysis indicated a possibility of them being runaways.

- For sample 2 we first attempted to obtain a GOSSS spectrum (Sect. 2.2). This confirmed the nature of some of the objects as O stars and discarded others. For the rest we searched the literature for photometry and conducted a CHORIZOS analysis to estimate their (Sect. 3.3). This also confirmed some as O stars and discarded others. Finally, objects without GOSSS spectral types or a CHORIZOS analysis were also discarded.
- For sample 3 we also first attempted to obtain a GOSSS spectrum, which confirmed the nature of part of the sample and discarded another part. For the rest we searched the literature for spectral classifications and retained only those coming from references with a proven record of coincidence with GOSSS spectral types (see Maíz Apellániz et al. 2004b and GOSSS-I for discussions on this issue). The rest were discarded. We did not attempt a CHORIZOS analysis for BA supergiants, as the main contaminant of the sample are BA stars of lower luminosity, which are difficult to distinguish based on photometry alone.

Finally, we also excluded some objects that are too close to us, as the method used to find runaway stars can yield false positives in that case, although we retained some close known runaways such as ζ Oph. The total number of objects that were discarded for one reason or another is given in Table 1. Clearly, sample 3 is the most mixed of the three, and we found the strongest mixed objects to be the alleged A supergiants: Simbad contains many objects with such classifications that are later found to be

[1] The GOSSS spectra are being gathered with six facilities: the 1.5 m Telescope at the Observatorio de Sierra Nevada (OSN), the 2.5 m du Pont Telescope at Las Campanas Observatory (LCO), the 3.5 m Telescope at the Observatorio de Calar Alto (CAHA), and the 2.0 m Liverpool Telescope (LT), the 4.2 m *William Herschel* Telescope (WHT), and the 10.4 m Gran Telescopio Canarias (GTC) at the Observatorio del Roque de los Muchachos (ORM). Of these, the LT is a recent addition.

[2] We found that ALS 18 929, which we had previously claimed as O9.7, is a B0 star after obtaining better data, see below. There are two other similar cases that we plan to publish soon and two other stars in GOSSS-III that we suspect may be sdO. Of these five objects, only ALS 18 929 has HIPPARCOS or TGAS proper motions and is therefore relevant for this paper.

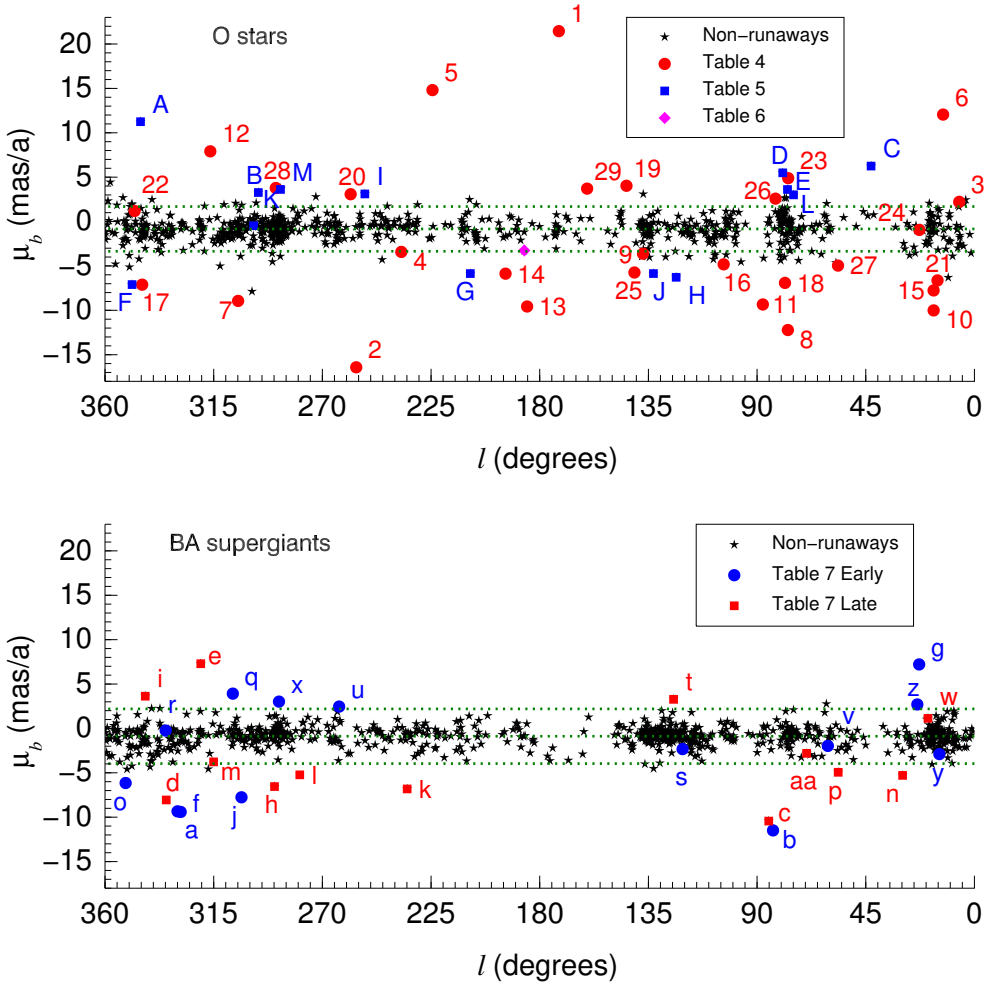

Fig. 1. Observed proper motion in Galactic latitude for the O stars (*top panel*) and the BA supergiants (*bottom panel*). Different colors and symbols are used to identify the runaway candidates in Tables 4–7, and the IDs in these tables are also shown. The dotted green lines represent the functions and 2σ deviations used to detect runaway candidates. The vertical scales are the same in both panels to facilitate comparison.

something else. Our strategy is designed to minimize the number of false positives at the risk of increasing the number of false negatives because the latter will likely be found in the next few years using future *Gaia* data releases. In other words, in order to eliminate (or at least largely reduce) our noise, we are forced to reduce our signal.

After establishing how we selected our sample, we now describe how we detected the runaway-star candidates. Ideally, to identify runaway stars, one computes the 3D motions of the stars and compares them to the expected velocities at their location using a Galactic rotation model. This requires knowledge not only of the proper motions, but also of the distances and radial velocities. Since we do not have precise measurements of the latter two for most of the sample, we are forced to follow a modification of the 2D proper-motion-only method used by Moffat et al. (1998) to identify Wolf–Rayet (WR) and O-star runaways with HIPPARCOS.

For all of the objects in our samples, the proper motions in RA (μ_α) and declination (μ_δ) were transformed into their equivalents in Galactic latitude (μ_b) and longitude (μ_l). Then, a robust mean for μ_b (reflecting the solar motion in the vertical direction), $\langle\mu_b\rangle$, and a robust standard deviation, σ_{μ_b}, were calculated for both the O stars (samples 1+2) and the BA supergiants (sample 3). For μ_l we robustly fitted a functional form $f(l) = a_0 + a_1 \cos l + a_2 \cos 2l$, and we also calculated the robust standard deviation, σ_{μ_l}, from the fit. Results are shown in Table 8 and Figs. 1 and 2.

To detect runaway stars, we computed the normalized difference (in standard deviations) of the difference between the observed proper motions and the fitted ones, that is,

$$\Delta = \sqrt{\left(\frac{\mu'_b}{\sigma_{\mu_b}}\right)^2 + \left(\frac{\mu'_l}{\sigma_{\mu_l}}\right)^2},$$

where $\mu'_b = \mu_b - \langle\mu_b\rangle$ and $\mu'_l = \mu_l - f(l)$ are the corrected proper motions, and sorted the results from largest to smallest. The cut in Δ is the same in both cases and was empirically established at 3.5 by comparing our results with those of the 3D method of Tetzlaff et al. (2011), who used a threshold of 28 km s^{-1} for the peculiar velocity of a runaway star. This 2D method is simpler than a full computation of the 3D velocities and has the advantage of being self-contained and therefore less prone to errors introduced by the required external measurements in the 3D method (distances and radial velocities). However, it can yield false positives and negatives, which we analyze later on.

2.2. GOSSS spectra

To confirm the spectral type of the runaway candidates, one should ideally obtain good-quality spectroscopy. That is what we did for the 25 objects in Table 2 as part of the GOSSS project. The spectrograms are shown in Figs. 3–5. The spectral classification was made using MGB (Maíz Apellániz et al. 2012, 2015a) and a new grid of spectroscopic standards that extends

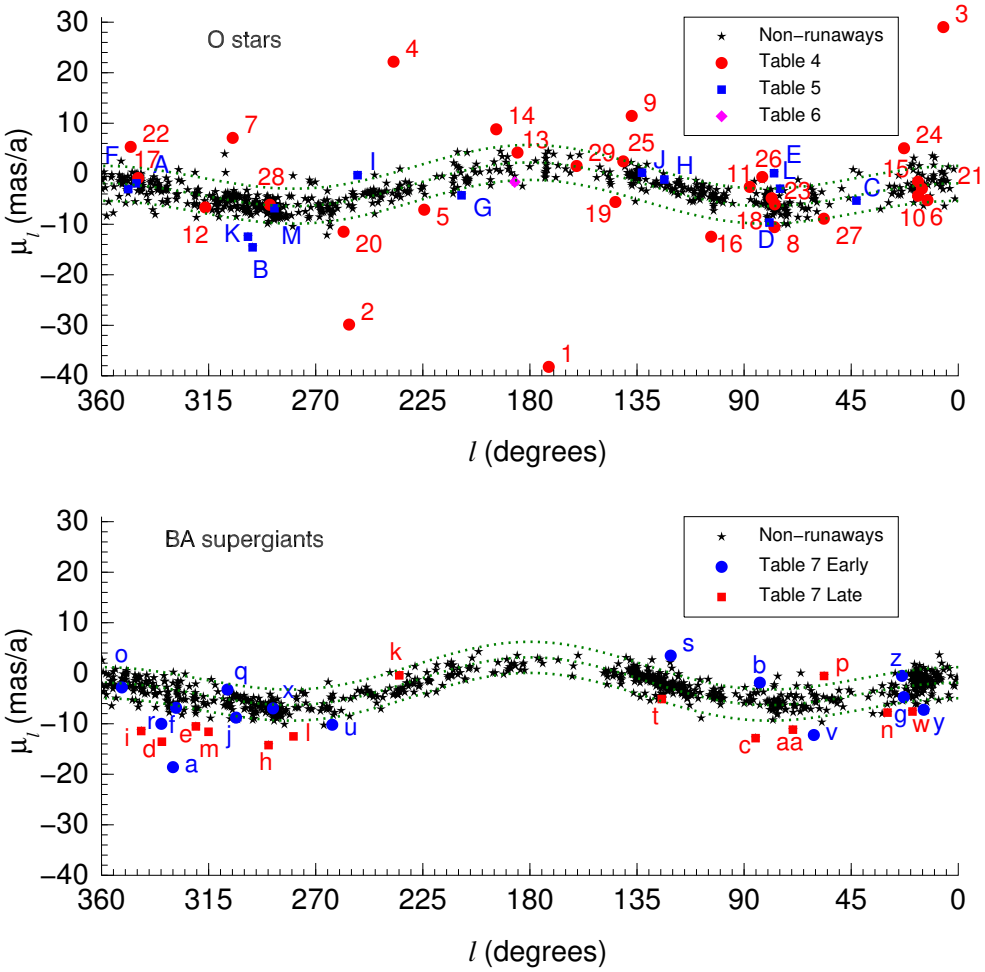

Fig. 2. Observed proper motion in Galactic longitude for the O stars (*top panel*) and the BA supergiants (*bottom panel*). Different colors and symbols are used to identify the runaway candidates in Tables 4–7, and the IDs in these tables are also shown. The dotted green lines represent the functions and 2σ deviations used to detect runaway candidates. The vertical scales are the same in both panels to facilitate comparison.

to A0 for luminosity classes II to V and to A7 for supergiants (Maíz Apellániz et al., in prep.). The new spectrograms are presented in Figs. 3–5, and the new spectral types are given in Table 2. Each of the new stars is discussed in the results section. The addition of the new objects leaves the GOSSS statistics with a total of 594 O stars, 20 other early-type stars, and 11 late-type stars. The spectrograms and spectral types are available from the Galactic O-Star Catalog (GOSC; Maíz Apellániz et al. 2004a; Maíz Apellániz et al. 2017a) web site. GOSC has recently been moved to a new URL[3], but the old one[4] will be kept as a mirror, at least temporarily.

2.3. Photometry and CHORIZOS

Unfortunately, we were not able to obtain good-quality spectroscopy for all of our runaway candidates in time for the publication of this paper. For the stars without spectral types, we collected photometry from the literature and used CHORIZOS (Maíz Apellániz 2004) to estimate their effective temperatures. For details on how this is done, we refer to Maíz Apellániz et al. (2014), where we explain how this procedure can be carried out without significant biases, and to Maíz Apellániz et al. (2018), where we use photometry similar to the one in this paper to measure extinction for a large sample of Galactic stars (see Arias et al. 2006; Maíz Apellániz et al. 2007, 2015b; Simón-Díaz et al. 2015a; Damiani et al. 2017 for further examples). The procedure for this paper is detailed below.

- We did not include in the analysis objects without accurate photometry at either sides of the Balmer jump (Johnson UB or Strömgren uv), because it is not possible to adequately measure the effective temperature ($T_{\rm eff}$) of OBA stars for these objects.
- We used the Milky Way grid of Maíz Apellániz (2013) and the family of extinction laws of Maíz Apellániz et al. (2014).
- For each star we left $T_{\rm eff}$, $E(4405-5495)$ (amount of extinction), and R_{5495} (type of extinction) as free parameters, and $\log d$ (logarithmic distance) as a dummy parameter. The luminosity class (LC) was fixed.

The results of our CHORIZOS analysis are shown in Table 3 and are discussed in Sect. 2.4. We emphasize that the identifications as O stars based on photometry should be taken with care until a spectroscopic confirmation is obtained.

2.4. WISE imaging

For each of the new runaway candidates, we searched for the dust emission from possible bow shocks in the WISE W3 and W4 images. In most cases we did not find any sign of one. However, some of them have bow shocks or other interesting structures that we show in Fig. 6 as RGB mosaics using the W4+W3+W2 channels.

3. Runaway candidates

In this section we provide information about each of the new objects that we have identified as possible runaways. Given the differences in our previous knowledge about the runaway

[3] http://gosc.cab.inta-csic.es
[4] http://gosc.iaa.es

Table 2. New GOSSS spectral classifications sorted by Galactic longitude.

Name	GOSSS ID	R.A. (J2000)	Decl. (J2000)	ST	LC	Qual.	Second	Paper
ALS 4962	GOS 010.85+03.27_01	18:21:46.166	−21:06:04.42	ON5	I	fp	...	...
HD 171 012	GBS 014.52−04.38_01	18:33:10.096	−18:22:06.18	B0.2	Ia	...	...	...
BD −08 4617	GOS 022.79+00.99_01	18:29:14.330	−08:33:40.91	O8.5	III	(n)	...	...
BD −08 4623	GBS 022.88+00.66_01	18:30:34.797	−08:38:03.69	B0.5:	Ia:	...	...	...
HD 161 961	GBS 023.64+12.90_01	17:48:36.856	−02:11:46.29	B0.5	Ib	...	...	...
67 Oph	GBS 029.73+12.63_01	18:00:38.716	+02:55.53.63	B5	Ib	...	...	...
ALS 18 929	GBS 042.79+10.57_01	18:31:01.379	+13:30:12.85	B0	V	...	...	III
HD 161 695	GAS 056.40+26.94_01	17:45:40.235	+31:30:16.84	A0	Ib	...	...	...
HD 190 066	GBS 060.69−04.54_01	20:02:22.102	+22:09:05.26	B0.7	Iab	...	...	...
ALS 11 244	GOS 079.36+02.61_01	20:22:37.775	+41:40:29.15	O4.5	III	(n)(fc)p	...	...
69 Cyg	GBS 083.39−09.96_01	21:25:47.025	+36:40:02.59	B0.2	Iab	...	...	...
HD 215 733	GBS 085.16−36.35_01	22:47:02.508	+17:13:59.00	B1	Ib	...	...	...
κ Cas	GBS 120.84+00.14_01	00:32:59.987	+62:55:54.43	BC0.7	Ia	...	...	...
HD 8065	GAS 124.57+15.96_01	01:23:45.801	+78:43:33.81	A0	Iab	...	...	...
ρ Leo AB	GBS 234.89+52.77_01	10:32:48.671	+09:18:23.71	B1	Ib	Nstr	...	...
CPD −34 2135	GOS 252.40−00.04_01	08:13:35.361	−34:28:43.93	O7.5	Ib	(f)p	...	...
GP Vel	GBS 263.06+03.93_01	09:02:06.860	−40:33:16.90	B0.5	Ia	...	...	...
HD 94 909	GBS 287.96+01.94_01	10:56:24.465	−55:33:04.85	B0	Ia	...	...	...
HD 86 606	GBS 289.82−13.13_01	09:56:09.735	−71:23:21.49	B1	Ib	...	...	...
AB Cru	GOS 298.47+04.41_01	12:17:37.122	−58:09:52.44	O8	III	...	BN0.2: Ib:	...
HD 115 842	GBS 307.08+06.83_01	13:20:48.339	−55:48:02.49	B0.5	Ia	...	...	...
HD 156 359	GBS 328.68−14.52_01	17:21:18.725	−62:55:05.36	B0	Ia	...	...	...
HD 150 898	GBS 329.98−08.47_01	16:47:19.657	−58:20:29.19	B0	Ib	...	...	...
CPD −50 9557	GBS 334.87−02.73_01	16:39:07.728	−50:54:08.29	B0	Ib	...	...	...
HD 167 756	GBS 351.47−12.30_01	18:18:40.156	−42:17:18.22	B0.2	Ib	...	...	...

Notes. GOS/GAS/GBS stands for Galactic O/B/A star. The last column indicates which GOSSS paper (if any) the star was included in. The information in this table is also available in electronic form at the GOSC web site (http://gosc.cab.inta-csic.es).

character of the objects in this paper, we divided them into three categories for the sake of clarity: [a] runaways known before Paper I, [b] objects described as runaways for the first time in paper I, and [c] runaway candidates not in Paper I. Each category is presented in the next three subsections.

3.1. O-type runaways known before Paper I

The O stars that were known to be runaways before Paper I was published are listed in Table 4. Many of the stars are very bright, as evidenced by the fact that almost half of this sample has no TGAS proper motions. A list of references is provided for each object. The list is not intended to be complete, as that would occupy too much space (the list includes some of the first objects identified as runaway stars), but includes the first reference to the runaway character of each object that we found. We discuss this sample later on when we discuss the completeness.

All of the objects in Table 4 were presented in GOSSS I+II+III (we refer to these papers for a brief description of each star) except for BD −08 4617 (=ALS 9668 = LS IV −08 7), which is added to the GOSSS main catalog here. It was classified as O8.5 V: by Morgan et al. (1955). Our spectrogram in Fig. 3 coincides with their spectral subtype, but assigns a giant luminosity class and an (n) rotation index.

3.2. New runaways from Paper I

The stars identified as runaways for the first time in Paper I are given in Table 4. Each one is briefly described in this subsection, ordered by decreasing Δ or likelihood of being a runaway from their corrected proper motions.

HD 155 913 (=CPD −42 7710 = ALS 4407). GOSSS II classified this star as O4.5 Vn((f)), but cautioned that it is an SB2 according to OWN data (Barbá et al. 2010, 2017), so the width could be caused by an unresolved orbital motion in the GOSSS spectrogram. Aldoretta et al. (2015) also detected a visual companion. The proper motion of the star points away from the young stellar cluster NGC 6822, located half a degree away and the likely source of this runaway star. No bow shock is visible in the WISE images, but the region of the sky is quite crowded because of its location.

HD 104 565 (=CPD −57 5199 = ALS 2572). This nitrogen-deficient star was classified as OC9.7 Iab in GOSSS-II. HD 104 565 is 4° above the Galactic Plane and moving away from it and toward the east. Its proper motion points away from Cen OB1, which lies ∼8° away and is a possible origin for this runaway.

ALS 18 929 (=LSE 107 = Tyc 1036-00450-1). This object was given an O9.7 spectral subtype in GOSSS III with no luminosity class because of the discrepancy between the He/He and Si/He criteria. With the help of new data, we have reanalyzed the spectral classification and determined that B0 V is more appropriate, as Si III λ4552 is stronger than He II λ4542, see Fig. 4. Therefore, we move this object from the main GOSC catalog (Galactic O stars) to supplement 2 (other Galactic early-type stars). It is still likely to be a runaway, as it is a massive star

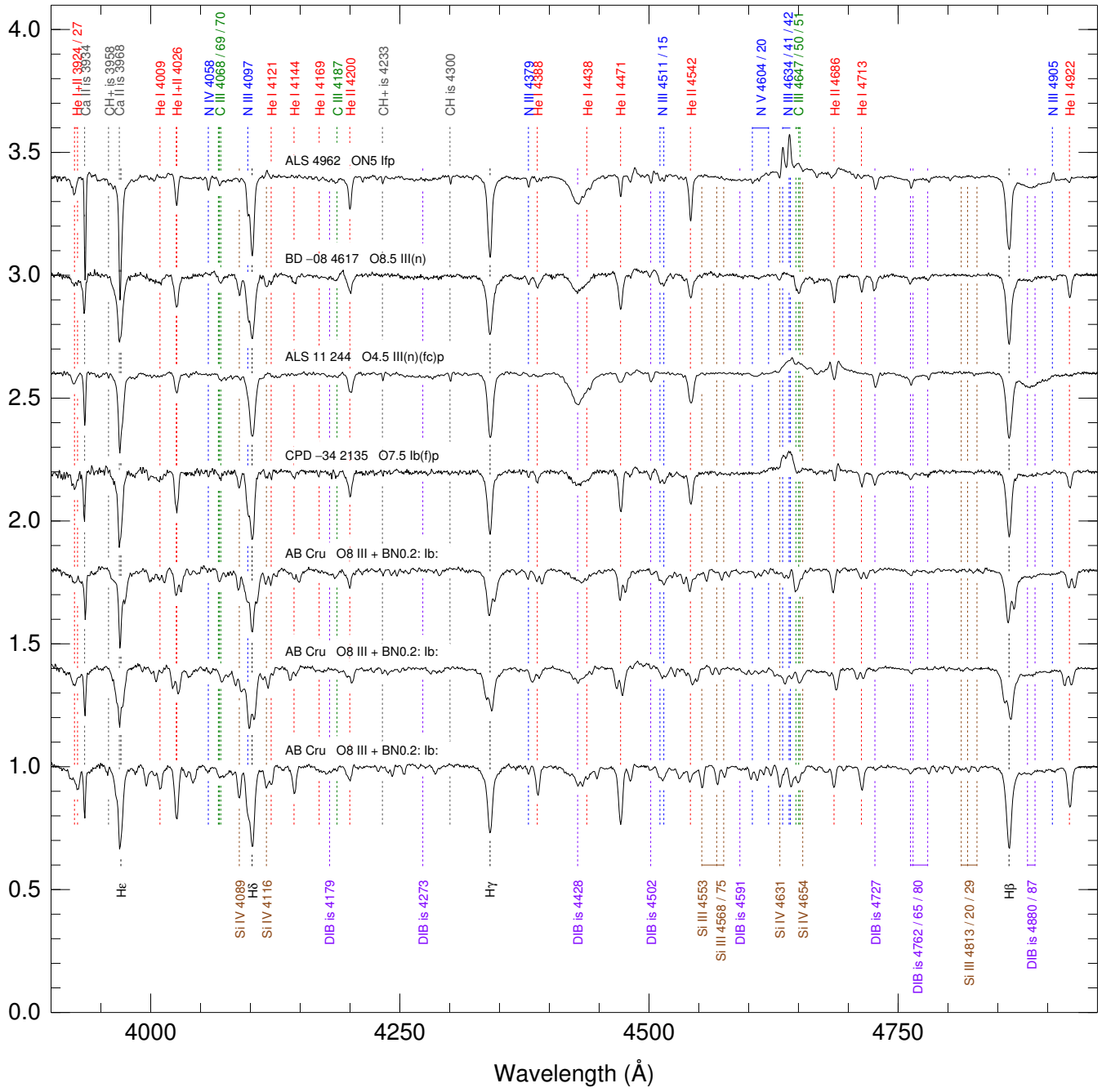

Fig. 3. GOSSS rectified spectrograms for the O stars in Table 2 sorted by Galactic longitude. For the SB2 AB Cru, three different orbital phases are shown.

located 10.°6 off the Galactic Plane and moving away from it in a direction close to perpendicular.

ALS 11 244 (=LS III +41 20). Comerón & Pasquali (2012) classified this star as O5 If. The spectrogram in Fig. 3 indicates a similar spectral subtype (O4.5) but a lower luminosity class of III, as He II λ4686 is not clearly in emission. Instead, it shows the double emission peak surrounding an absorption line characteristic of Onfp stars (see GOSSS-I). It also has C III λ4647–50–52 comparable to N III λ4634–40–42, hence the (fc) suffix in the classification (Walborn et al. 2010). Based on its proper motion, the most likely origin for this runaway star is the OB association Cyg OB2, located ∼2° away.

HDE 229 232 AB (=BD +38 4070 = ALS 11 296 = LS II +38 79). GOSSS-III classified this star as O4 V:n((f)). The object has a bright visual companion (Aldoretta et al. 2015) and is an SB1 (Williams et al. 2013). Based on its proper motion, the most likely origin of this runaway star is the young cluster NGC 6913, located ∼40′ away, but we note that HDE 229 232 AB is much earlier (hence, likely more massive) than the cluster turnoff (Negueruela 2004). Some warm dust is visible in the WISE images around HDE 229 232 AB (Fig. 6), but it does not appear to originate in a bow shock.

HD 155 775 (=V1012 Sco = CPD −38 6750 = ALS 3995). GOSSS-II classified this object as O9.7 III(n) and Malkov et al. (2006) indicated that it is an eclipsing binary. It is located close

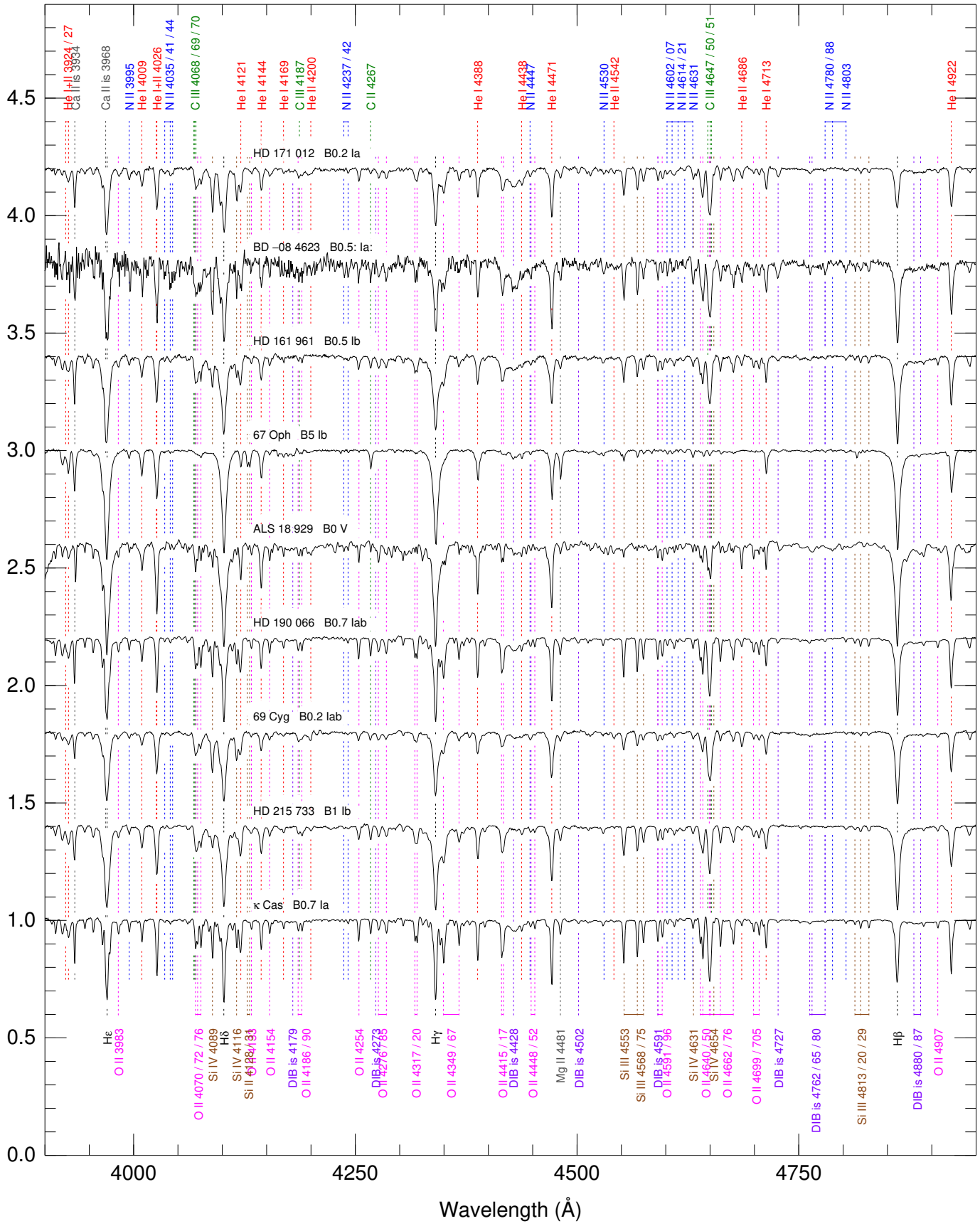

Fig. 4. GOSSS rectified spectrograms for the B stars in Table 2 sorted by Galactic longitude.

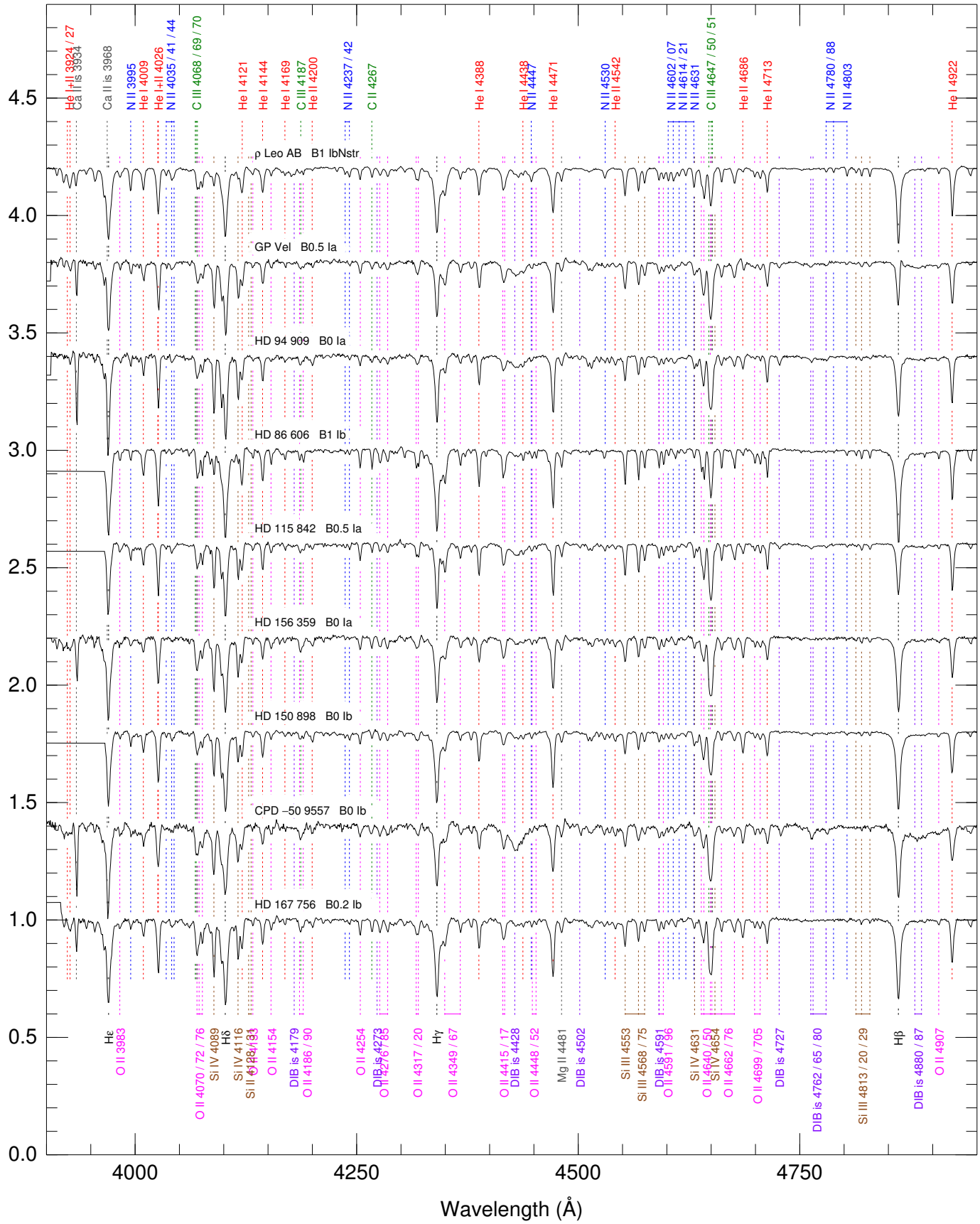

Fig. 4. continued.

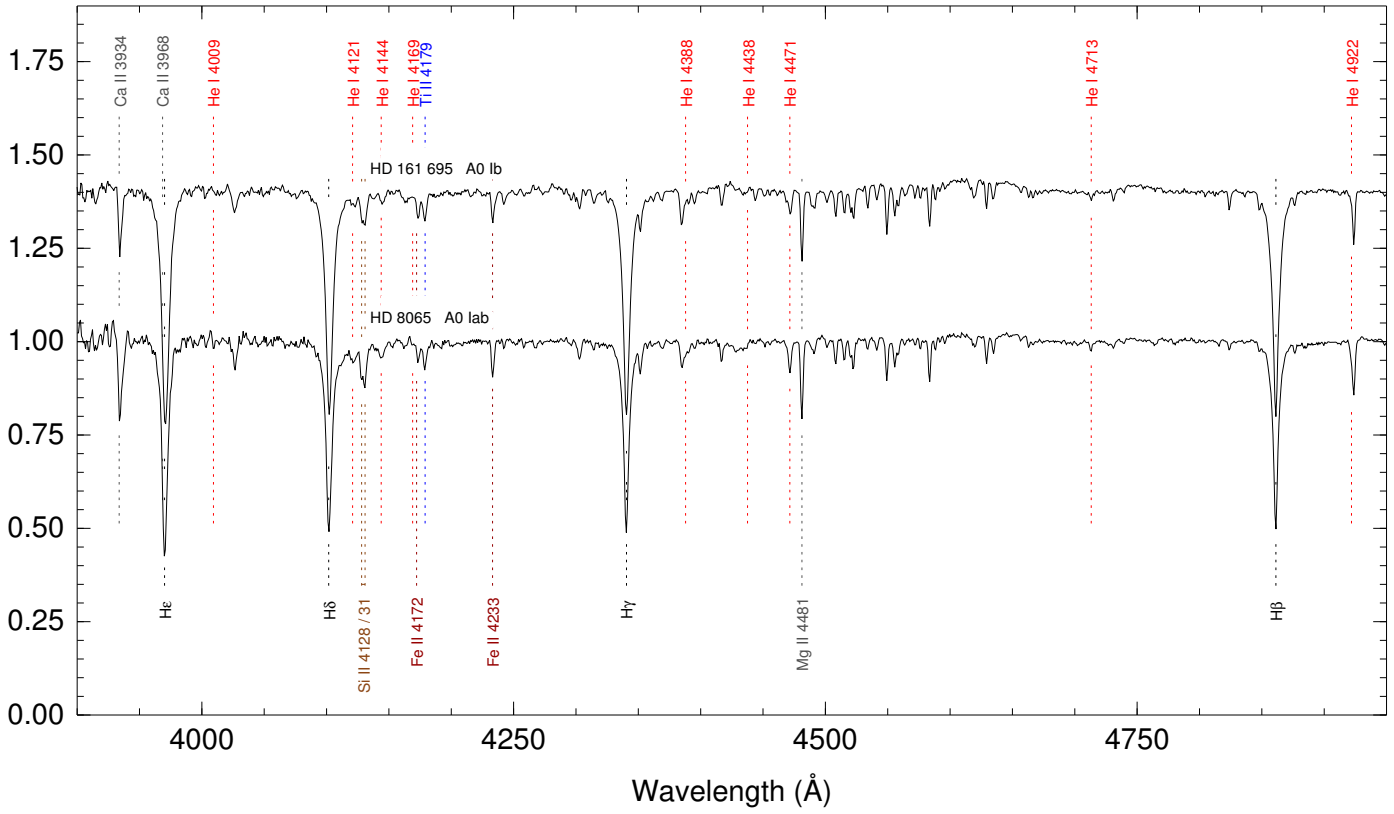

Fig. 5. GOSSS rectified spectrograms for the A stars in Table 2 sorted by Galactic longitude.

Table 3. Results of the CHORIZOS runs.

Name	R.A. (J2000)	Decl. (J2000)	Phot.	$T_{\rm eff}$ (kK)	LC	$E(4405-5495)$	R_{5495}	Conclusion
CPD −57 3781	10:46:11.507	−58:39:12.39	J2GT	$39.3^{+7.1}_{-6.9}$	5.0	$0.825^{+0.019}_{-0.025}$	$3.64^{+0.12}_{-0.11}$	Likely O
CPD −72 1184	11:58:59.966	−73:25:48.37	J2TS	$32.4^{+5.9}_{-2.6}$	5.0	$0.198^{+0.035}_{-0.037}$	$3.66^{+0.72}_{-0.54}$	Likely O, possibly early B
CPD −63 2886	13:39:35.390	−63:39:41.74	J2GT	$42.0^{+5.6}_{-6.9}$	5.0	$1.306^{+0.025}_{-0.025}$	$3.16^{+0.06}_{-0.08}$	Likely O
HDE 322 987	17:18:39.102	−37:20:16.79	J2GT	$41.1^{+6.1}_{-6.8}$	5.0	$1.200^{+0.019}_{-0.025}$	$3.24^{+0.08}_{-0.06}$	Likely O
HDE 315 927	17:31:57.315	−29:38:36.96	J2GTS	$39.5^{+6.8}_{-5.5}$	5.0	$1.156^{+0.013}_{-0.019}$	$3.04^{+0.06}_{-0.05}$	Likely O

Notes. The photometry (Phot.) column gives the bands included in each run with the same nomenclature as in Maíz Apellániz et al. (2018), i.e., J for Johnson *UBV*, 2 for 2MASS $JHK_{\rm S}$, G for *Gaia G*, T for *Tycho*-2 *BV*, and S for Strömgren *uvby*.

to the Galactic Plane and moving away from the open cluster ASCC 88, which could be its origin. The WISE image (Fig. 6) shows a weak bow shock consistent with the direction of the corrected proper motion, but we note that the region is quite crowded (Kobulnicky et al. 2016). The *Herschel* 160 μm band also shows a small cavity around the star consistent with the bow shock structure.

HD 46 573 (=BD +02 1295 = ALS 9029 = LS IV +02 10). GOSSS-I classified this star as O7 V((f))z. The object is moving away from the Galactic Plane, and tracing back its trajectory, we arrive at NGC 6822, an H II region with a young cluster and a potential origin for the runaway. We note that another runaway, HD 47 432, is present nearby. We do not detect it with our method (i.e., it is one of our false negatives), but it was identified as a runaway by Tetzlaff et al. (2011). The trajectories of both runaways intersect at almost a right angle at the location of Collinder 110, but this open cluster is too old to have produced such young stars, so it is likely a chance superposition (we will check this with *Gaia* DR2, nonetheless). The WISE image shows a strong bow shock consistent with the corrected TGAS proper motion (Fig. 6, see Paper I and Kobulnicky et al. 2016).

BD +60 134 (=ALS 6405 = LS I +61 173). GOSSS III obtained a spectral classification of O5.5 V(n)((f)) for this star. BD +60 134 is in the neighborhood of several OB associations in Cassiopeia. Based on its proper motion, Cas OB7 appears to be the most likely origin, but we note that the star is earlier (hence, likely more massive) than any star in the association.

CPD −34 2135 (=ALS 1007). Garrison et al. (1977) classified this star as O7 III. We find a slightly later spectral subtype and a brighter luminosity class, O7.5 Ib(f)p. The p suffix is assigned for its incipient P-Cygni profile in He II λ4686, see Fig. 3. CPD −34 2135 is located very close to the Galactic Plane and moving in a diagonal direction

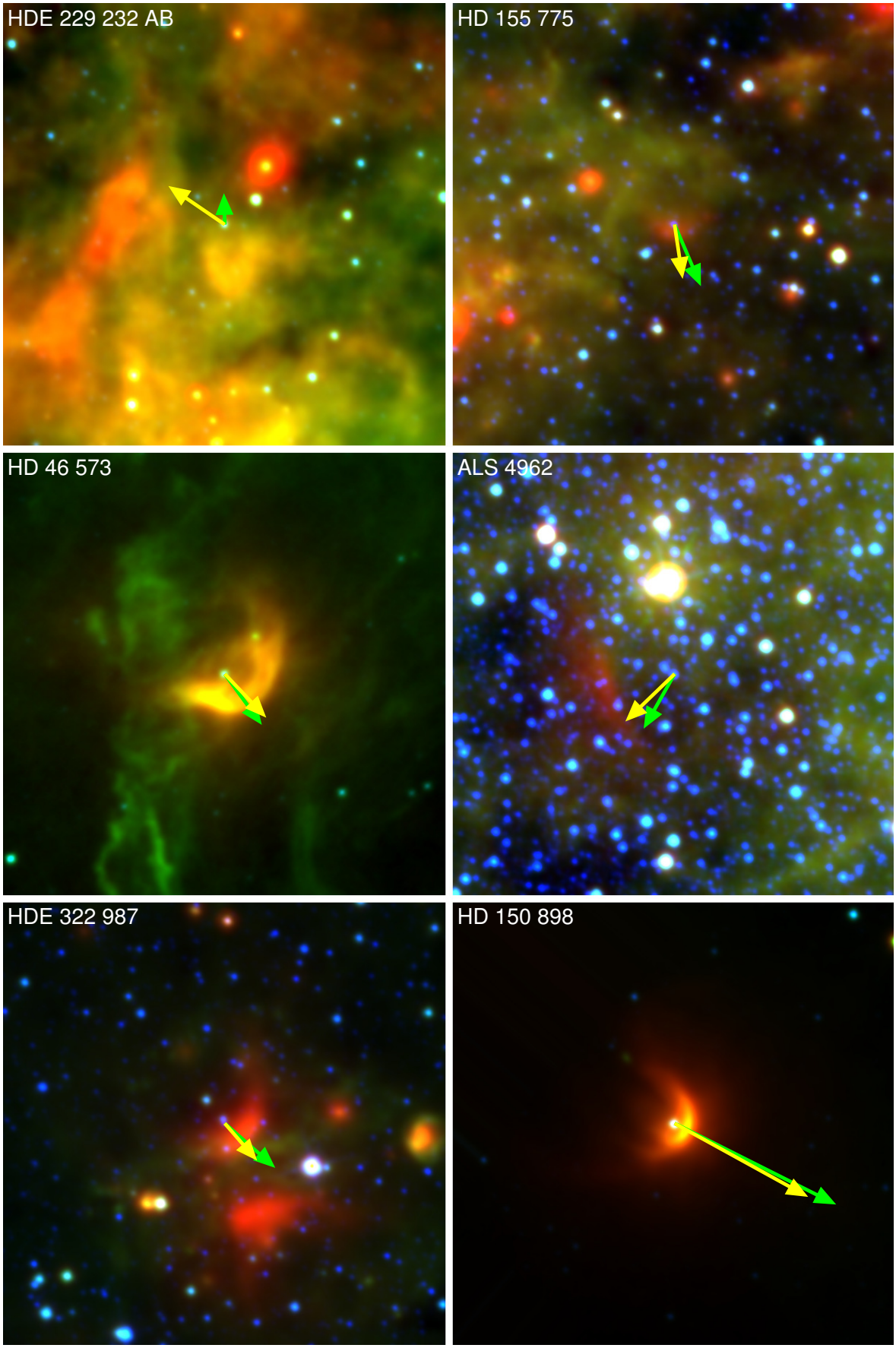

Fig. 6. WISE W4+W3+W2 RGB mosaics for 12 of the runaway candidates sorted by their order of appearance. Each field is 14′ × 14′ and is oriented with Galactic (not equatorial) north toward the top and Galactic east toward the left. In each mosaic the runaway candidate is at the center, and the arrows show the original (green) and the corrected proper motion (yellow).

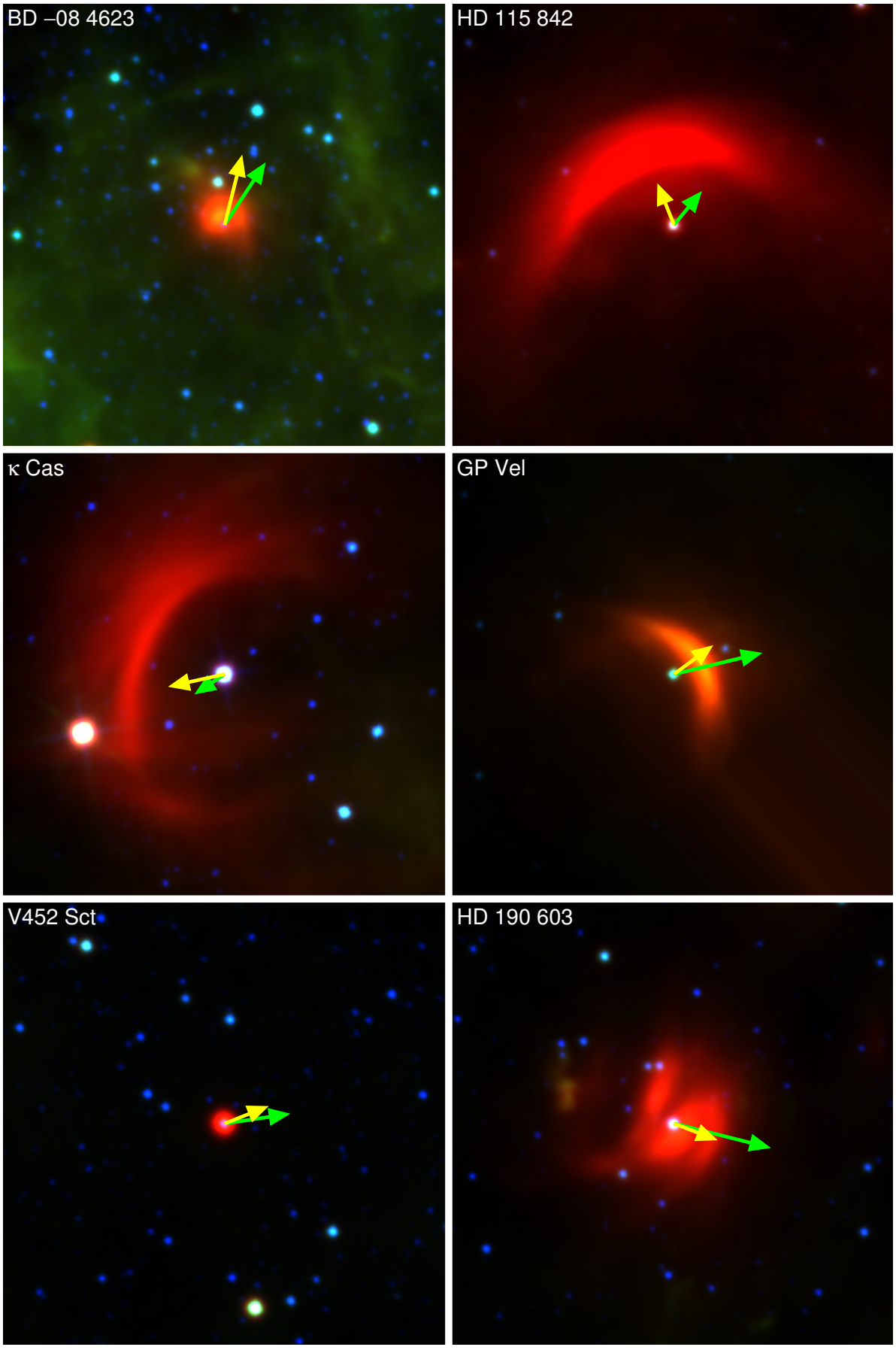

Fig. 6. continued.

Table 4. Previously known O-type runaway stars from Table 1 in Paper 1.

ID	Name	μ'_b	μ'_l	T/H	Ref.
1	AE Aur	22.29	−40.33	T	B54, B01, H01, L12
2	ζ Pup	−15.58	−24.49	H	C74, N97, H01, S08
3	ζ Oph	3.05	31.00	H	B61, G79, H01, T10
4	μ Col	−2.59	25.43	H	B54, B01, H01, T11
5	HD 57 682	15.64	−5.63	T	M04, G12, S14, P15
6	HD 157 857	12.89	−3.05	H	B61, M04, S08, T11
7	HD 116 852	−8.11	12.43	H	C74, M98, M04, S08
8	Y Cyg	−11.38	−4.17	T	G85, M05a, S08, T11
9	HD 17 520 A	−2.78	12.72	H	M04, D12, S14
10	V479 Sct	−9.17	−2.00	T	R02, M12, M16
11	68 Cyg	−8.51	3.71	H	B61, W89, S08, T11
12	HD 124 979	8.74	−2.27	T	T11, D12, S14
13	HD 36 879	−8.74	2.01	T	M04, M05, M16
14	HD 41 997	−5.03	7.00	T	C74, M98, M04, S08
15	BD −14 5040	−6.93	0.80	T	G08, P15, M16
16	λ Cep	−3.99	−7.08	H	B61, H01, G11, v88
17	HD 152 623 AaAbB	−6.28	1.44	H	S96, M05b, M09, M16
18	HD 201 345	−6.08	1.57	H	C74, d05, S08, T11
19	α Cam	4.87	−5.23	H	B61, d85, S91, M05b
20	HD 75 222	3.91	−5.92	T	H01, S08, T11, S14
21	HD 175 876	−5.80	−0.67	H	S96, S08, T11, S14
22	HD 153 919	2.03	7.47	T	S75, A01, M04, S08
23	HD 192 281	5.72	0.34	T	C74, M04, S08, T11
24	BD −08 4617	−0.10	7.76	T	M04
25	HD 14 633 AaAb	−4.91	3.24	H	S78, B05, S08, T11
26	HD 195 592	3.42	5.77	T	C74, v95, S08, T11
27	9 Sge	−4.12	−3.46	T	S82, N97, M04, S08
28	HD 96 917	4.61	0.09	T	T11, S14
29	ξ Per	4.54	0.14	H	B61, H01, T11, S11

Notes. The list is sorted by Δ, the normalized deviation from the mean latitude and longitude proper motions for their Galactic longitude. An ID is provided for each star in order to identify it in Figs. 1 and 2. The T/H flag indicates the origin of the proper motions (TGAS or HIPPARCOS, respectively). Some relevant references are listed in the last column. See Tables 5–7 for the remaining runaways.

References. A01: Ankay et al. (2001), B54: Blaauw & Morgan (1954), B61: Blaauw (1961), B01: Bagnuolo et al. (2001), B05: Boyajian et al. (2005), C74: Cruz-González et al. (1974), d85: de Vries (1985), d05: de Wit et al. (2005), D12: de Bruijne & Eilers (2012), G79: Gull & Sofia (1979), G08: Gvaramadze & Bomans (2008), G11: Gvaramadze & Gualandris (2011), G12: Grunhut et al. (2012), G85: Gies & Bolton (1985), H01: Hoogerwerf et al. (2001), L12: López-Santiago et al. (2012), M98: Moffat et al. (1998), M04: Mdzinarishvili (2004), M05a: Mdzinarishvili & Chargeishvili (2005), M05b: Meurs et al. (2005), M09: Mason et al. (2009), M12: Moldón et al. (2012), M16: Maíz Apellániz et al. (2016), N97: Noriega-Crespo et al. (1997), P15: Peri et al. (2015), R02: Ribó et al. (2002), S75: Sutantyo (1975), S78: Stone (1978), S82: Stone (1982), S91: Stone (1991), S96: Sayer et al. (1996), S08: Schilbach & Röser (2008), S11: Sota et al. (2011), S14: Sota et al. (2014), T10: Tetzlaff et al. (2010), T11: Tetzlaff et al. (2011), v88: van Buren & McCray (1988), v95: van Buren et al. (1995), W89: Wisotzki & Wendker (1989).

with respect to it. Tracing back its proper motion, a possible origin in the young star clusters in Canis Majoris is found.

HD 12 323 (=BD +54 441 = ALS 6886 = LS I +55 22). This nitrogen-rich star was classified as ON9.2 V in GOSSS II. Musaev & Chentsov (1989) found it to be a spectroscopic binary and Kendall et al. (1995) identified it as a blue straggler. This object is over 5 degrees to the south of the Galactic Plane and moving away from it. Its proper motion points toward the OB associations Per OB1 and Cas OB8 as possible origins.

AB Cru (=HD 106 871 = CPD −57 4397 = ALS 2639). Garrison et al. (1977) classified this star as O8 Vn, but other sources identify it as a B star. One possible reason for the discrepancies is that the spectrum of this object is highly variable due to its eclipsing binarity (Popper 1966). Here we used GOSSS spectra to determine that it is an O8.5 III + BN0.2: Ib: system (Fig. 3), one of the very few known combinations of an O star and a B supergiant in a short-period binary[5]. The B supergiant has a significant N enrichment. We are using GOSSS and OWN (Barbá et al. 2010, 2017) spectroscopy to determine the orbit. AB Cru is 4.°4 above the Galactic Plane and moving westward almost parallel to it. If it has been ejected from a system to the east, then its motion is apparently being already bent back toward the Galactic Plane[6]. One candidate for its origin is the Cen OB1 association, ∼6° away.

[5] But note that the luminosity class of the B star is uncertain.

[6] Throughout this paper, we say that a runaway star is moving toward the Galactic Plane when this occurs on the plane of the sky, that is, when μ'_b and b have opposite signs. As we do not have information on the radial velocity and the distance, we do not know if this is also true in terms of true 3D velocity.

Table 5. New O- and B0-type runaway star candidates from Table 1 in Paper 1.

ID	Name	μ'_b	μ'_l	T/H
A	HD 155 913	12.08	0.35	T
B	HD 104 565	4.10	−8.66	T
C	ALS 18 929[a]	7.08	−0.99	T
D	ALS 11 244	6.33	−3.24	T
E	HDE 229 232 AB	4.44	6.49	T
F	HD 155 775	−6.26	−0.93	T
G	HD 46 573	−5.03	−4.77	T
H	BD +60 134	−5.44	2.01	T
I	CPD -34 2135	3.95	4.76	T
J	HD 12 323	−5.02	2.07	T
K	AB Cru	0.36	−6.69	T
L	HD 192 639	3.84	3.39	T
M	HD 94 024	4.46	−0.52	T

Notes. The list is sorted by Δ, the normalized deviation from the mean latitude and longitude proper motions for their Galactic longitude. An ID is provided for each star in order to identify it in Figs. 1 and 2. The corrected proper motions are in mas a^{-1}. The T/H flag indicates the origin of the proper motions (TGAS or HIPPARCOS, respectively). See Tables 4, 6, and 7 for the remaining runaways. [(a)]Not an O star, but a B0 V.

HD 192 639 (=BD +36 3958 = ALS 10 996 = LS II +37 26). GOSSS-I classified this star as O7.5 Iabf (it is an O7.5 Iab standard). It is located within the Cyg OB1 association moving northward away from the Galactic Plane. In paper I we proposed the open cluster Dolidze 4 as a possible origin, but this is uncertain, as the corrected proper motion traces back to a point close to the cluster, but not within it.

HD 94 024 (=CPD −57 3856 = ALS 1952). GOSSS-II classified this star as O8 IV. OWN data (Barbá et al. 2010, 2017) indicate that this system is an SB1. HD 94 024 is moving away from the Carina Nebula association, its likely origin, located 2° to the south.

3.3. Objects not in Paper I

In this subsection we describe the runaway candidates that were not discussed in Paper I, dividing them into O stars and BA supergiants.

3.3.1. O stars

The (spectroscopically confirmed or not) O stars in this subsection are listed in Table 6. Each one is briefly described in this subsubsection, ordered by decreasing Δ.

HDE 315 927 (=CPD −29 4760 = ALS 4200). Vijapurkar & Drilling (1993) classified this star as O5 III, but we do not have GOSSS data to verify it. The CHORIZOS run (Table 3) yields a $T_{\rm eff}$ consistent with that spectral classification and a moderate extinction with an R_{5495} close to the canonical value of 3.1. We didnot find any previous identifications of HDE 315 927 as a runaway star. Tracing back its proper motion leads to several clusters in Sgr in the direction of the Galactic Center as its possible origin.

CPD −72 1184 (=ALS 2557). This object has been classified as a late-type O (O9 III, Wramdemark 1980) or as an early-type B (B0 III; Kilkenny 1974). We do not have GOSSS data to verify the spectral classification, and the CHORIZOS run (Table 3) yields a $T_{\rm eff}$ consistent with a late-type O but without excluding the possibility of being an early-type B and a low extinction. Therefore, we tentatively leave it here with the intention of confirming the spectral classification in the near future. Kilkenny (1974) identified it as a runaway star, and de Bruijne & Eilers (2012) measured a radial velocity of −218 km s^{-1}. CPD −72 1184 is located 11° to the south of the Galactic Plane and moving in a direction almost perpendicular to it. It could have originated in the region between Centaurus and Crux. This is the only object in this subsubsection with a HIPPARCOS instead of a TGAS proper motion.

Table 6. O-type runaway star candidates not in Paper 1.

ID	Name	μ'_b	μ'_l	T/H	P/S	Known
α	HDE 315 927	5.27	−6.46	T	P	no
β	CPD −72 1184	−7.04	0.37	H	P	yes
γ	ALS 4962	−5.47	5.66	T	S	no
δ	CPD −63 2886	0.63	9.02	T	P	no
ε	HDE 322 987	−4.29	−3.73	T	P	no
ζ	CPD −57 3781	4.58	−0.11	T	P	yes
η	HD 74 920	0.17	−6.12	T	S	no

Notes. The list is sorted by Δ, the normalized deviation from the mean latitude and longitude proper motions for their Galactic longitude. An ID is provided for each star in order to identify it in Figs. 1 and 2. The corrected proper motions are in mas a^{-1}. The T/H flag indicates the origin of the proper motions (TGAS or HIPPARCOS, respectively). The P/S flag indicates whether the identification of the star as being of O type is photometric or spectroscopic, respectively. The Known column indicates whether the runaway character of the object has been identified previously. See Tables 4, 5, and 7 for the remaining runaways.

ALS 4962. This star is potentially the most interesting object in this subsubsection. It has received little previous attention, but Kilkenny (1993) classified it as O9 Ia. The GOSSS spectrum confirms its supergiant nature (but note that He II λ4686 is not fully in emission and is closer to a P-Cygni profile) and brings the spectral subtype to a much earlier O5. O5 is established, as usual, from the He II λ4542/He I λ4471 ratio, but that leaves us with N III+IV+V absorption lines significantly stronger than expected, hence the ON designation and the p suffix, as the ON phenomenon is not expected to appear in early/mid-supergiants. It is also possible that the spectrum is a composite of an earlier O and a later O star, but even under this assumption it would be hard to reach the intensity of the nitrogen absorption lines. ALS 4962 shows strong atomic, molecular, and DIB ISM absorption lines, an indication of strong extinction. We found no previous indication of its runaway nature in the literature. A faint structure in the WISE W4 band is consistent with a bow shock that is slightly offset from the direction of the corrected proper motion (Fig. 6). Tracing back its motion leads to the western part of the Sgr OB1 association near the location of M20 as a possible origin.

CPD −63 2886 (=ALS 3140). Vijapurkar & Drilling (1993) classified this star as O9.5 Ib, but we do not have GOSSS data to verify it. The CHORIZOS run (Table 3) yields a $T_{\rm eff}$ consistent with that of an O star, likely even earlier than O9.5, and a relatively high extinction with an R_{5495} close to the canonical value of 3.1. We did not find any previous identifications of CPD −63 2886 as a runaway star. It is moving eastward in a

direction parallel to the Galactic Plane away from the Cen OB1 association, a possible origin.

HDE 322 987 (=CPD −37 7076 = ALS 4059). This object appears as O7 in Goy (1973) and as O5 V in Vijapurkar & Drilling (1993), but we do not have GOSSS data to verify the spectral classification. The CHORIZOS run (Table 3) yields a $T_{\rm eff}$ consistent with those classifications along with a moderate extinction with an R_{5495} close to the canonical value of 3.1. We found no previous indication of its runaway nature in the literature. The WISE mosaic shows extended emission in the region expected for a bow shock (Fig. 6; Kobulnicky et al. 2016), but the region is crowded and other sources are present, so an alternative explanation such as a PDR cannot be discarded. Regarding possible origins, this is a crowded region where it is difficult to select an origin without further information. One of the candidates is the H II region RCW 126.

CPD −57 3781 (=ALS 1887). Crampton (1971) classified this star as O8 and Vijapurkar & Drilling (1993) as O7 V(n), but we do not have GOSSS data to verify the spectral classification. The CHORIZOS run (Table 3) yields a $T_{\rm eff}$ consistent with these classifications and a moderate extinction with a value of R_{5495} significantly higher than the canonical value. This object is moving away form the Carina Nebula association, located 1° away, its more likely origin. CPD −57 3781 is the ionizing star of the optical H II region RCW 52, whose shape and alignment is consistent with being at least partially a bow shock created by this runaway star, a fact first noted by Cappa et al. (2005).

HD 74 920 (=CPD −45 2978 = ALS 1148). GOSSS-II classified this star as O7.5 IVn. It was not included in paper I as it was just below the threshold there, but with the slightly modified parameters here, it is just above it. We did not find any previous identifications of this object as a runaway star. HD 74 920 is moving westward in a direction nearly parallel to the Galactic Plane within the Vel OB1 association. It could have originated in one of the H II regions toward the east, such as RCW 38 or RCW 40.

3.3.2. BA supergiants

The BA supergiants in this subsection are listed in Table 7. Each one is briefly described in this subsubsection, ordered by decreasing Δ.

HD 150 898 (=CPD −58 693 = ALS 15 035). GOSSS data yield a spectral type of B0 Ib for this star, which has previously been identified as a runaway (Hoogerwerf et al. 2001; Tetzlaff et al. 2011). A clear bow shock is visible in the WISE mosaic (Fig. 6). Its proper motion traces back to the Ara-Scorpius region of the Galactic Plane 15–20° away.

69 Cyg (=HD 204 172 = BD +36 4557 = ALS 14 838 = V2157 Cyg). This object has a spectral type of B0.2 Ib in GOSSS data and has previously been identified as a runaway (Hoogerwerf et al. 2001; Mdzinarishvili & Chargeishvili 2005). Tracing back its proper motion yields a likely origin in the Cygnus region ∼10° away.

HD 215 733 (=BD +16 4814 = ALS 14 757). GOSSS data yield a spectral type of B1 Ib for this star, which has previously been identified as a runaway (Tetzlaff et al. 2011). Based on its proper motion, a possible origin is in the Lac OB1 or Cep OB2 associations 30–40° away.

Table 7. BA-supergiant runaway star candidates.

ID	Name	μ'_b	μ'_l	T/H	Known	E/L
a	HD 150 898	−8.46	−15.37	H	yes	E
b	69 Cyg	−10.61	4.40	T	yes	E
c	HD 215 733	−9.56	−6.61	H	yes	L
d	γ Ara	−7.18	−10.62	H	no	L
e	HD 119 608	8.17	−6.49	H	unclear	L
f	HD 156 359	−8.53	−3.51	H	yes	E
g	BD −08 4623	8.09	−2.03	T	no	E
h	HD 86 606	−5.67	−8.07	T	yes	L
i	θ Ara	4.51	−9.11	H	yes	L
j	HD 112 272	−6.88	−3.36	T	yes	E
k	ρ Leo AB	−5.94	2.00	H	yes	L
l	ϕ Vel	−4.35	−6.20	H	no	L
m	HD 125 288	−2.89	−7.10	H	no	L
n	67 Oph	−4.41	−4.59	H	no	L
o	HD 167 756	−5.27	−0.80	H	no	E
p	HD 161 695	−4.06	4.87	T	no	L
q	HD 115 842	4.80	1.92	T	no	E
r	CPD −50 9557	0.64	−7.17	T	no	E
s	κ Cas	−1.45	6.52	H	yes	E
t	HD 8065	4.16	−2.62	T	unclear	L
u	GP Vel	3.34	−4.52	T	yes	E
v	HD 190 066	−1.09	−6.54	T	yes	E
w	V452 Sct	2.01	−5.10	T	yes	L
x	HD 94 909	3.90	−0.74	T	no	E
y	HD 171 012	−2.01	−5.01	H	yes	E
z	HD 161 961	3.58	2.23	T	no	E
aa	HD 190 603	−1.93	−5.04	T	no	L

Notes. The list is sorted by Δ, the normalized deviation from the mean latitude and longitude proper motions for their Galactic longitude. An ID is provided for each star in order to identify it in Figs. 1 and 2. The corrected proper motions are in mas a^{-1}. The T/H flag indicates the origin of the proper motions (TGAS or HIPPARCOS, respectively). The Known column indicates whether the runaway character of the object had been identified previously. The last column indicates whether the spectral type is E(arly, from B0 to B0.7) or L(ate, B1 or later). See Tables 4–6 for the remaining runaways.

γ Ara (=HD 157 246 = CPD −56 8225 = ALS 15 048). This object has a spectral type of B1 Ib in GOSSS data and we did not find any reference to its runaway character. It is one of the closest objects in our list, but both its HIPPARCOS and spectroscopic parallaxes place it beyond 300 pc. Its proper motion traces back to the Scorpius region of the Galactic Plane 20–25° away.

HD 119 608 (=BD −17 3918 = ALS 14 746). Morgan et al. (1955) classified this star as B1 Ib, but we did not observe it with GOSSS. It is not clear whether this object has previously been identified as a runaway: McEvoy et al. (2017) indicated that it is one, but used Martin (2004) as a reference for this claim. Martin (2004) reported, however, that HD 119 608 is a post-asymptotic giant branch (PAGB) star instead of a runaway B supergiant, while Szczerba et al. (2007) later described it not as a PAGB, which unpublished data from the IACOB project (Simón-Díaz et al. 2015b) also indicate. HD 119 608 is located far above the Galactic Plane, and its possible origin could have been the Sgr region of the Galactic Plane, ∼60° away.

HD 156 359 (=CPD −62 5531 = ALS 16 942). GOSSS data yields a spectral type of B0 Ia for this star, which has

previously been identified as a runaway (House & Kilkenny 1978; Mdzinarishvili 2004). Tracing back its corrected proper motion leads to Ara OB1 as a possible origin.

BD −08 4623 (=ALS 9685 = LS IV −08 8). GOSSS yields a spectral type of B0.5: Ia:, with the uncertainty in the classification arising from the relatively low S/N of the data (see Fig. 4). There are also indications that the spectrum might be composite: we will observe it again to obtain better data. We found no indication of its runaway nature in the literature. The WISE mosaic (Fig. 6) shows an asymmetrical warm-dust region around the star as opposed to a clear bow shock (although the position is as expected from the corrected proper motion), and the star has apparently created a bubble around it (Simpson et al. 2012). BD −08 4623 is in the Sct region of the Galactic Plane moving toward the north, so it is likely that its origin is nearby.

HD 86 606 (=CPD −70 953 = ALS 14 941). This object has a spectral type of B1 Ib in GOSSS data and was identified as a runaway star by Tetzlaff et al. (2011). According to the corrected proper motion, a possible origin is Cen OB1, ∼18° away.

θ Ara (=HD 165 024 = CPD −50 10538 = ALS 15 053). Hiltner et al. (1969) classifies it as B2 Ib, but Simbad lists other classifications ranging from B0.5 Iab to B1 II. We did not obtain GOSSS data for this star, which is one of the closest targets in our sample. It was identified as a runaway star by Tetzlaff et al. (2011). It is already falling back toward the Galactic Plane, so that its origin is hard to trace based only on the corrected proper motion.

HD 112 272 (=DW Cru = CPD −63 2454 = ALS 2834). Morgan et al. (1955) classified this star as B0.5 Ia, but we did not obtain a GOSSS spectrum to confirm it. It was identified as a runaway star by Tetzlaff et al. (2011). It is located within the Cen OB1 association, moving away from its center.

ρ Leo AB (=HD 91 316 AB = BD +10 2166 AB = ALS 14 811 AB). GOSSS yields a spectral classification of B1 IbNstr for this nitrogen-enhanced star, which was first considered a runaway star by Keenan & Dufton (1983). ρ Leo AB is located far away from the Galactic Plane and already falling back toward it. The AB designation is due to the existence of an elusive bright companion (there are several historical references that failed to detect it) that according to Tokovinin et al. (2010) is 1.5 magnitudes dimmer than the primary (hence contributing significantly to the spectrum) and separated by 46 mas. There are also claims in the literature that the object is a spectroscopic binary, but an extensive spectroscopic monitoring performed by the IACOB project (Simón-Díaz et al. 2015b) clearly demonstrates that the spectroscopic variability is produced by stellar oscillations and rotational modulation of a non-spherically symmetric wind (see also Aerts et al. 2018).

ϕ Vel (=HD 86 440 = CPD −53 3075 = ALS 14 940). Hiltner et al. (1969) classified this star as B5 Ib, but we did not obtain a GOSSS spectrum to confirm it. There is no previous reference to its runaway nature in the literature. It is located close to the Galactic Plane, and one possible origin is the open cluster ASCC 58, 3° away.

HD 125 288 (=v Cen = CPD −55 5984 = ALS 14 996). Hiltner et al. (1969) classified this star as B6 Ib, but we did not obtain a GOSSS spectrum to confirm it. We did not find any previous reference to its runaway nature. It is moving westward and already falling back toward the Galactic Plane.

67 Oph (=HD 164 353 = BD +02 2186 = ALS 14 022). The GOSSS spectral classification for this star is B5 Ib, and there is no previous mention of its runaway nature in the literature. It is already falling back toward the Galactic Plane.

HD 167 756 (=CPD −42 8359 = ALS 14 536). We classify this star as B0.2 Ib with GOSSS data. We found no previous reference to its runaway nature. It is moving in a direction close to perpendicular to the Galactic Plane, with one possible origin in NGC 6357 or its neighborhood.

HD 161 695 (=BD +31 3090). The GOSSS spectrum yields a classification of A0 Ib for this star, consistent with previous results. HD 161 695 is not only located far from the Galactic Plane (27°), but is also one of the runaways in this paper that is falling back toward the Galactic Plane. Therefore, tracing back its origin is not possible without additional distance and velocity information. Somewhat surprisingly for a sixth-magnitude supergiant at its location, we did not find any references to its runaway nature in the literature.

HD 115 842 (=CPD −55 5504 = ALS 3038). The GOSSS spectral classification for this star is B0.5 Ia, and there is no previous mention of its runaway nature in the literature. The WISE mosaic (Fig. 6) shows a large and strong bow shock consistent with the corrected proper motion. A possible origin for this runaway is Cen OB1, located 7° away.

CPD −50 9557 (=ALS 3689). We classify this star as B0 Ib with GOSSS data, and we found no previous reference to its runaway nature in the literature. It is moving westward below the Galactic Plane, so that its origin is difficult to ascertain.

κ Cas (=HD 2905 = BD +61 102 = ALS 6258). GOSSS yields a spectral classification of BC0.7 Ia for this object, which was previously known to be a runaway (van Buren et al. 1995; Tetzlaff et al. 2011). The WISE mosaic (Fig. 6) shows a large and strong bow shock consistent with the corrected proper motion. κ Cas is moving eastward close to the Galactic Plane within the region of the sky shared by the Cas OB4 and Cas OB14 OB associations. It is interesting to note that this is a carbon-enhanced B supergiant. Several other runaways in this paper have CNO peculiarities, and Sk −67 2 in the LMC was recently discovered by Lennon et al. (2017) to be another case of a carbon-enhanced runaway B supergiant/hypergiant.

HD 8065 (=BD +77 49). This supergiant has published spectral subtypes that range from B9 to A2, but a comparison of the GOSSS spectrum with the A0 supergiant standards indicates that it is an A0 Iab. We list the previously known status of this little-studied star as "unclear" since the only relevant information we found in the literature is a note in Table 1 of Bidelman (1988) that says "has this high-latitude B9 Iab star escaped from h and χ Persei?" The answer to that question from TGAS data is that it is indeed a possibility: the corrected proper motion traces back to the Perseus double cluster 20° away (crossing the Galactic Plane in the meantime), but with such a long distance one would need a careful 3D analysis to confirm the suspicion.

GP Vel (=HD 77 581 = Vel X-1 = CPD −40 3072 = ALS 1227). The GOSSS spectral classification for this star is B0.5 Ia. with an incipient P-Cygni profile in Hβ that is not strong enough to warrant a Ia+ luminosity class. GP Vel is a high-mass X-ray binary in an 8.9 day orbit (McClintock et al. 1976) that was previously known to be a runaway star (Kaper et al. 1997; Tetzlaff et al. 2011). The WISE W4 mosaic (Fig. 6) shows a clear bow shock consistent with the corrected proper motion. Tracing back its trajectory leads to a possible origin in the eastern part of the Vel OB1 association.

HD 190 066 (=BD +21 4027 = ALS 10 740 = LS II +22 20). We classify this star as B0.7 Iab based on GOSSS data. It was previously known to be a runaway (Tetzlaff et al. 2011). It is moving westward below the Galactic Plane with a possible origin in the Cygnus region.

V452 Sct (=BD −13 5061 = ALS 5107 = LS IV −13 82). We did not observe this object with GOSSS, but the spectrum published by Miroshnichenko et al. (2000) indicates it is an A0 Ia+. This paper also indicates that it is a likely runaway star. This is one of the more distant objects in our sample, as it is likely beyond the Galactic Center. The WISE mosaic shows an excess in this band that is consistent with being a point source centered on the star, therefore it is likely caused by the IR excess studied by Miroshnichenko et al. (2000) and not by a bow shock. V452 Sct is already falling back toward the Galactic Plane.

HD 94 909 (=V526 Car = CPD −56 4016 = ALS 2036). The GOSSS spectral classification for this star is B0 Ia. To our knowledge, it has not previously been identified as a runaway star. It is moving away from the Galactic Plane in a nearly perpendicular direction, with a possible origin in the Carina Nebula association, 2° away, or a point slightly toward the east.

HD 171 012 (=V4358 Sgr = BD −18 4994 = ALS 5086). The GOSSS spectral classification for this star is B0.2 Ia, and it was previously known to be a runaway (Tetzlaff et al. 2011). One possible origin lies in the Sct OB associations, 10–12° away.

HD 161 961 (=BD −02 4458 = ALS 9353 = LS IV −02 5). The GOSSS spectrum yields a classification of B0.5 Ib for this star, which has not previously been identified as a runaway. Tracing back its corrected proper motion leads to the Sct OB associations ∼15° away.

HD 190 603 (=V1768 Cyg = BD +31 3925 = ALS 1079 = LS II +32 15). We did not observe this object with GOSSS, but Lennon et al. (1992) gives a spectral classification of B1.5 Ia+ and the star was analyzed in detail by Clark et al. (2012). We found no prior references to its runaway character. The WISE mosaic (Fig. 6) shows an asymmetric nebula around it with a direction that is consistent with the corrected proper motion. The nebula does not have the typical shape of a bow shock, but this might be due to the extremely high mass-loss rate of this object (Lennon et al. 1992; Walborn et al. 2015), which could produce a more filled structure. HD 190 603 is moving westward close to the Galactic Plane, and its likely origin is in one of the Cygnus OB associations.

4. Analysis

4.1. Completeness

To check for false negatives in our list, we searched Tetzlaff et al. (2011) for runaway candidates with a high probability of having a peculiar velocity[7] ($P_{v_{\rm pec}} > 0.5$) that are missing in Table 4 but are present in our sample 1. Thirty-three objects are missing, but 30 of them were detected by Tetzlaff et al. (2011) based mainly on their radial velocities as they have (a) $P_{v_{\rm r,pec}} > P_{v_{\rm t,pec}}$ and (b) $P_{v_{\rm t,pec}} < 0.5$. Therefore, we would not expect them to be detected by our 2D method. Of the remaining three objects, one is HD 93 521, which has no TGAS data and is the Galactic O star with the highest latitude by far ($b = 52°$), which makes it difficult to detect with a 2D method that is optimized for objects near the Galactic Plane. The other two, HD 108 and HDE 227 018, have TGAS proper motions with significantly smaller uncertainties and are closer to the mean values than the HIPPARCOS values, which were used by Tetzlaff et al. (2011). Hence, a 3D reanalysis would likely reduce their $P_{v_{\rm t,pec}}$. We conclude that our method correctly picks up runaway stars with high tangential velocities, but misses some that are moving mostly in a radial direction, as expected. For O stars the 2D method detects approximately half of the stars that a 3D method would pick up, but the exact number is hard to evaluate given the differences between our sample 1 and that in Tetzlaff et al. (2011).

Objects that we identify as runaway stars, but that are not, are false positives. In their work on main-sequence B-type (i.e., lower mass) runaways, Silva & Napiwotzki (2011) described their efforts to clean their sample of hot evolved low-mass stars, in their case, blue horizontal branch (BHB) stars. For our higher-mass sample the expected fraction of such contaminants should be lower, as PAGB stars are the possible false detections (see Fig. 1 of Silva & Napiwotzki 2011), and this phase is much shorter than the BHB phase and only overlaps with our objects at the lower luminosity end. Another possible contaminant are sdO stars, but these objects are excluded by the GOSSS spectral classification (see footnote 3). Therefore, we expect our false positives (if they exist) to have other origins such as incorrect astrometric values. The final answer about the number of false positives will lie in future work, of course, but there is a good reason why the new 13 objects in sample 2 were not detected before as runaways. Eight of them do not have HIPPARCOS proper motions, and the remaining five were not included in Tetzlaff et al. (2011). Therefore, most of the runaway O candidates will probably be confirmed in the future, possibly as soon as *Gaia* DR2 data become available.

A completeness analysis for BA supergiants is more difficult than for O stars for three reasons:

- There is currently no whole-sky spectroscopic survey of B supergiants analogous to GOSSS for O stars and the fraction of false identifications is high, as it is easy to find lower-luminosity B stars that are misclassified as supergiants. Hence, the sample is poorly defined, and we are forced to reject a significant fraction of the potential runaways (Table 1) either because we have obtained a spectrum and found that the object was not a B supergiant or because there is no good-quality spectral classification in the literature.
- The situation is even worse for A supergiants. These are rare objects because of the speed at which massive stars cross this region of the Hertzsrpung–Russel diagram, and there are just a few classification standards in the literature.

[7] The peculiar velocity $v_{\rm pec}$ is the velocity of the object with respect to the average disk velocity at its location.

Table 8. Robust parameter fits for the O stars and BA supergiants.

Sp. ty.	$\langle\mu_b\rangle$	σ_{μ_b}	a_0	a_1	a_2	σ_{μ_l}
O	−0.83	1.26	−3.04	−2.07	3.21	1.73
BA I	−0.88	1.03	−2.72	−2.51	3.35	1.54

– Most previous runaway studies have paid decreasing attention to stars of O type (through early-B and late-B) to A supergiants, which makes it difficult to compare our results with previous ones.

Therefore, we can only extrapolate from the O-star case to estimate that Table 7 will contain a few false positives, but we cannot provide a number of expected false negatives.

4.2. Comparing runaway O stars and runaway BA supergiants

In this subsection we compare our results for O stars and BA supergiants and analyze their similarities and differences. We first consider the fit parameters for the mean proper motions in Table 8 and Figs. 1 and 2. The fits are very similar, and the differences between the top and bottom panels in each figure are hard to appreciate. The dispersions for O stars are only slightly larger. This result indicates that the bulk of both samples (i.e., the non-runaway stars have similar properties in terms of distances and kinematics, as expected given that during the lifetimes of BA supergiants they cannot travel far from their birth places (in a Galactic scale) unless they are ejected as runaways.

Next, we examine the distribution of stars by Galactic longitude in Fig. 7. The left panel shows the distributions of the whole samples: O stars and BA supergiants follow a similar pattern, with a marked concentration toward the inner Galaxy. The concentration is the result of the strong negative radial gradient in the density of massive stars in the Galaxy, which overcomes the likewise negative gradient in extinction in the local neighborhood (Maíz Apellániz et al. 2018). The overdensity of O stars with respect to BA supergiants in the second and seventh octants is caused by the presence of Cygnus and Carina, respectively, which are the two regions in the solar neighborhood with the highest concentrations of O stars. The opposite is seen in the third octant, mostly caused by the low-extinction supergiant-rich Perseus arm. The right panel shows the distributions of the runaway candidates. For O stars there appears to be little change, but for BA supergiants the concentration towards the inner Galaxy becomes significantly more marked: there are no runaway BA supergiants in the outer two octants, and only two are seen in the third and sixth octants. Even though numbers are relatively low, this is probably partially an extinction effect: in the inner Galaxy, extinction is significantly higher but also patchy and associated with star-forming regions (Maíz Apellániz et al. 2018). Runaway BA supergiants have more time to travel away from the birth places and find locations where the sightline is significantly less strongly extinguished, especially if the ejection velocity vector has a significant vertical component.

In Fig. 8 we analyze the relationship for runaway stars between Galactic latitude and its corrected proper motion in the absolute sense, $\mu'_{|b|}$, that is, μ'_b multiplied by the sign of b so that the quantity is positive if the star is moving away from the Galactic Plane and negative if it is falling back towards it. We have divided the BA supergiants into two subsamples: those with spectral subtypes B0-B0.7, and those with later spectral subtypes. Regarding b, we see that runaway O stars and runaway early-B supergiants have similar dispersions and with a mean close to zero (no preference for either Galactic hemisphere)[8]. This indicates that there are no large time-difference effects between these two groups: an early-B supergiant is older than a mid- or early-O dwarf, but that is not necessarily true if the comparison is made with a late-O dwarf, which evolves into an early-B giant (not supergiant). On the other hand, runaway later-type supergiants have a significantly higher dispersion in Galactic latitude, indicating that they have been able to travel farther away from the Galactic Plane because of their older average ages.

With respect to $\mu'_{|b|}$, we also see similarities between runaway O stars and runaway early-B stars: both have average values that indicate that they are more likely to be moving away from the Plane than falling toward it. The dispersion is higher for O stars, but this may be explained by the existence of some stars that are close to crossing the Galactic Plane for the first time because they have very recently been ejected (two good examples of this are AE Aur, Hoogerwerf et al. 2001, and HD 155 913). On the other hand, runaway later-type supergiants have an average value of $\mu'_{|b|}$ which is very close to zero: this indicates that enough flight time has passed for about half of them to start falling back toward the Galactic Plane.

Finally, we consider whether there are differences in the fraction of O stars and BA supergiants that are runaways. A direct reading of Table 1 gives a value of 5.7% fo the runaway fraction for O stars. However, as we described previously, a comparison with Tetzlaff et al. (2011) points toward an incompleteness close to one half, mostly due to the use of a 2D method for the detection of runaways. Therefore, a more realistic number would be in the 10–12% range. The number of BA supergiants in Table 1 is significantly lower than for O stars. There are at least three reasons why the real fraction is likely to be different:

– The use of a 2D method causes us to miss some runaways, that is, the same reason as for O stars.
– We have followed stricter criteria for the selection of BA supergiants, resulting in a higher fraction of discarded objects in Table 1. In some of these cases, we were able to confirm that the object was not a BA supergiant, but not in others.
– Runaway later-type supergiants are on average located farther away from their birthplaces and farther away from the Galactic Plane with respect to the other runaways. This facilitates detection, as the main limitation for observing Galactic massive stars is extinction, not distance (Maíz Apellániz et al. 2018).

The first two reasons favor an increase in the real fraction of runaway BA supergiants, but the last reason argues against it. When we assume that the first reason has a similar effect for supergiants as for O stars and that the last two cancel out (at least approximately), the real fraction of runaway supergiants is close to 6%, that is, lower than for O stars. However, this value is just an estimate that needs to be confirmed by better data in the form of a better sample selection and improved data.

4.3. Runaways and rotational velocity

Runaways produced by supernova explosions are expected to have high rotational velocities (Blaauw 1993), a characteristic that was verified by Hoogerwerf et al. (2001) for Galactic stars with a rather small sample and later on by Walborn et al. (2014) for 30 Doradus (see their Fig. 9). Here we can use the

[8] We recall that HD 93 521 is not included in the sample, but the addition of a single star would not change the result significantly.

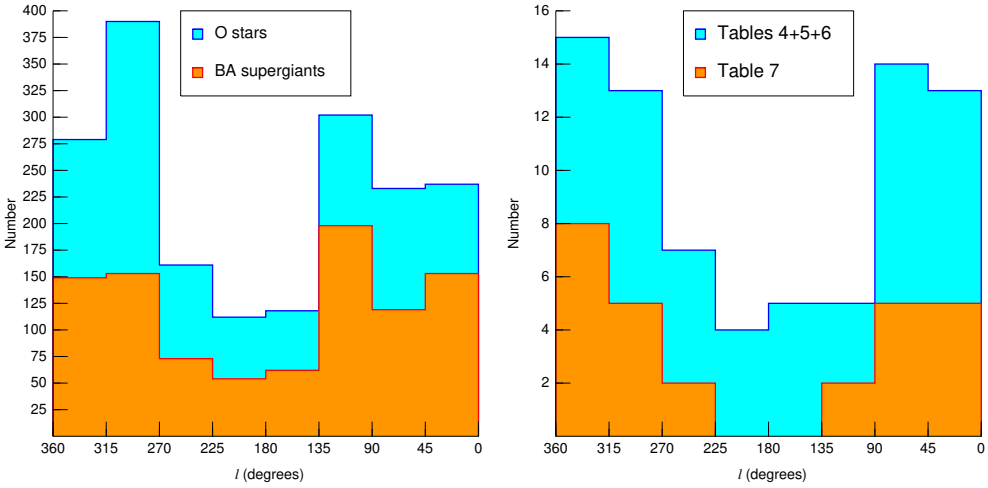

Fig. 7. Galactic longitude histograms for O stars (blue/cyan) and supergiants (red/orange). The *left panel* shows the whole sample, and the *right panel* presents the runaway candidates.

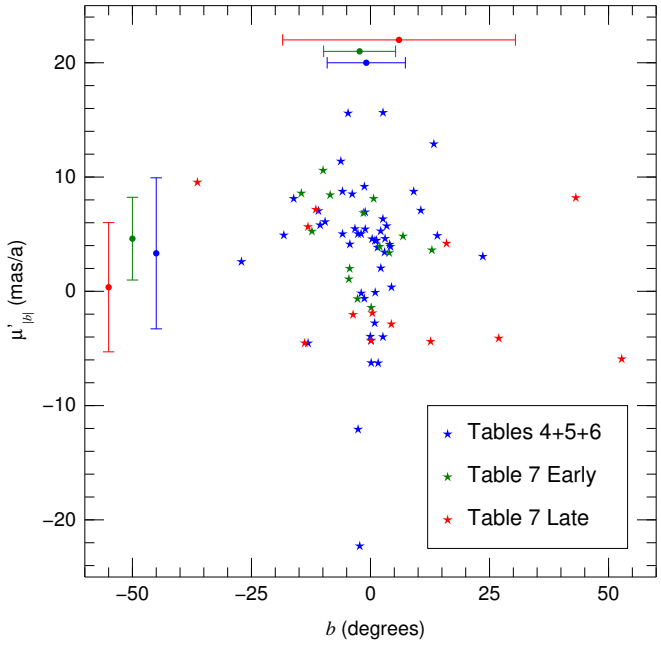

Fig. 8. Corrected latitude proper motions in the absolute sense (positive for motions away from the Galactic Plane, negative for falling-back motions) as a function of Galactic latitude for runaway O stars (blue), B0–B0.7 supergiants (green), and B1 and later-type supergiants (red). The error bars show the mean and standard distribution for each sample and coordinate.

homogeneous GOSSS sample of O stars to test whether runaway stars have higher rotational velocities than normal O stars. Each GOSSS spectral classification includes a line-width index that is empty for stars with low values of $v \sin i$ and is (*n*), *n*, or *nn* for stars with increasingly higher values of the projected rotational velocity[9]. More specifically, the line-width index measures the broadening of intrinsically narrow lines (metallic absorption lines are preferred over He I lines and those over He II lines), which is linked to rotation in most cases. However, some stars with apparently broad lines are instead unresolved (in velocity) spectroscopic binaries. Over time, we have been repeating GOSSS observations of stars with broad lines in order to resolve such cases and give independent spectral classifications to each component, but some few contaminants might still be present in the sample.

We present in Table 9 the statistics on the line-width index for the 590 O stars in GOSSS I+II+III (the control group) and the 44 O stars identified as runaways in this paper with GOSSS spectral classifications. We note that most of the objects in the second group (along with the undetected O-type runaways) are included in the first group. For the control group, 26.2 ± 1.8% (155/590) of the objects have non-empty line-width indices (fast rotators), while for the O runaways, the corresponding fraction is 46.5 ± 7.6% (20/43). Considering that we expect to be missing about half of the O-type runaways, the GOSSS sample is expected to contain close to 500 non-runaways, of which ∼115 (∼19%) will have non-empty line-width indices (if the characteristics of the undetected runaways are similar to those of the detected ones). Therefore, we can conclude that Galactic runaway O stars rotate significantly faster on average than their non-runaway counterparts.

We also note that there is a significant difference between O supergiants (understood as luminosity classes II to Iab) and O stars in lower luminosity classes. Among the former, we find 3 fast rotators and 11 slow rotators, while among the latter, there are 17 fast rotators and 12 slow rotators. This is likely to be an age effect, as the rotational velocity is expected to decrease due to mass loss with a spin-down timescale of a few Ma (Lau et al. 2011). This result indicates that fast rotators are a majority of our runaway sample at ejection, although we note that statistics may be biased in either direction: some fast rotators will not be identified as such due to their low value of sin *i* and some apparent fast rotators may actually be SB2s (e.g., HD 155 913). On the other hand, some runaways are the product of a multiple ejection (e.g., AE Aur and μ Col, Hoogerwerf et al. 2000) and others, such as Y Cyg (Harmanec et al. 2014) and AB Cru (this paper), are close binaries. In both situations, the alternative scenario (a dynamical encounter in a compact stellar cluster) is required to explain their origin. Therefore, it seems that both scenarios contribute to the population, but more runaways in our sample appear to be produced in supernova explosions, although better statistics are needed to confirm this claim. On the other hand, the study of Silva & Napiwotzki (2011) did not find such a prevalence of fast rotators but their sample was composed of main-sequence B stars i.e. of lower mass. Such a difference could be a mass effect, as it should be easier to eject a 5 $M_\odot$ at a high velocity in a dynamical interaction than a 25 $M_\odot$ one.

[9] The approximate values for $v \sin i$ for (*n*), *n*, and *nn* are 200, 300, and 400 km s^{-1}, respectively; see Walborn et al. (2014).

Table 9. Line-width index statistics for the GOSSS I+II+III O-star sample and the O stars identified as runaways in this paper with GOSSS spectral classifications.

Sample	Total	Empty	(*n*)	*n*	*nn*
GOSSS I+II+III	590	435	106	40	9
O runaways	43	23	14	5	1

5. Summary

We have searched for Galactic runaway stars using *Gaia* Data Release 1 and HIPPARCOS proper motions. The main results of this paper are summarized below.

- We presented 76 runaway star candidates, 17 of which had no clear previous identification, 2 are unclear cases, and 13 were presented as candidates for the first time in Paper I.
- Spectral classifications were assigned to 25 massive stars using GOSSS data, and their spectrograms are included.
- We provide photometry-based $T_{\rm eff}$ estimates for 5 stars and present WISE imaging for 12 runaway candidates.
- The 2D method we used is estimated to detect approximately half of the runaways in the sample.
- We detected differences in the distribution of runaway B1 and later-type supergiants compared to earlier runaways, and we ascribe the differences to an age effect.
- Tentatively, there appear to be fewer runaway BA supergiants than runaway O stars.
- Runaway O stars rotate on average faster than normal O stars. The supernova explosion scenario might contribute more objects to the population than the multi-body interaction scenario.

Acknowledgements. This work makes use of (a) data from the European Space Agency (ESA) mission *Gaia* (https://www.cosmos.esa.int/gaia), processed by the *Gaia* Data Processing and Analysis Consortium (DPAC; https://www.cosmos.esa.int/web/gaia/dpac/consortium) whose funding is provided by national institutions, in particular the institutions participating in the *Gaia* Multilateral Agreement; (b) data products from the Wide-field Infrared Survey Explorer (WISE), which is a joint project of the University of California, Los Angeles, USA, and the Jet Propulsion Laboratory/California Institute of Technology, USA, funded by the National Aeronautics and Space Administration of the USA; and (c) the SIMBAD database and the VizieR catalogue access tool, both operated at CDS, Strasbourg, France. J.M.A., A.S., and E.T.P. acknowledge support from the Spanish Government Ministerio de Economía, Industria y Competitividad (MINECO/FEDER) through grant No. AYA2016-75 931-C2-2-P. M.P.G. acknowledges support from the ESAC Trainee program. R.H.B. acknowledges support from the ESAC Faculty Council Visitor Program. S.S.-D., I.N., and E.T.P. acknowledge support from the Spanish Government Ministerio de Economía, Industria y Competitividad (MINECO/FEDER) through grant No. AYA2015-68 012-C2-1/2-P.

References

Aerts, C., Bowman, D. M., Simon-Diaz, S., et al. 2018, MNRAS, 476, 1234
Aldoretta, E. J., Caballero-Nieves, S. M., Gies, D. R., et al. 2015, AJ, 149, 26
Ankay, A., Kaper, L., de Bruijne, J. H. J., et al. 2001, A&A, 370, 170
Arias, J. I., Barbá, R. H., Maíz Apellániz, J., Morrell, N. I., & Rubio, M. 2006, MNRAS, 366, 739
Bagnuolo, Jr., W. G., Riddle, R. L., Gies, D. R., & Barry, D. J. 2001, ApJ, 554, 362
Barbá, R. H., Gamen, R. C., Arias, J. I., et al. 2010, RM&AC, 38, 32
Barbá, R. H., Gamen, R., Arias, J. I., & Morrell, N. I. 2017, in The Lives and Death-Throes of Massive Stars, eds. J. J. Eldridge, J. C. Bray, L. A. S. McClelland, & L. Xiao, IAU Symp., 329, 96
Bidelman, W. P. 1988, PASP, 100, 1084
Blaauw, A. 1961, Bull. Astron. Inst. Netherlands, 15, 265
Blaauw, A. 1993, in Massive Stars: Their Lives in the Interstellar Medium, eds. J. P. Cassinelli, & E. B. Churchwell, ASP Conf. Ser., 35, 207
Blaauw, A., & Morgan, W. W. 1954, ApJ, 119, 625
Boyajian, T. S., Beaulieu, T. D., Gies, D. R., et al. 2005, ApJ, 621, 978
Brown, A. G. A., Vallenari, A., Prusti, T., et al. 2016, A&A, 595, A2
Cappa, C., Niemela, V. S., Martín, M. C., & McClure-Griffiths, N. M. 2005, A&A, 436, 155
Clark, J. S., Najarro, F., Negueruela, I., et al. 2012, A&A, 541, A145
Comerón, F., & Pasquali, A. 2012, A&A, 543, A101
Crampton, D. 1971, AJ, 76, 260
Cruz-González, C., Recillas-Cruz, E., Costero, R., Peimbert, M., & Torres-Peimbert, S. 1974, Rev. Mex. Astron. Astrofis., 1, 211
Damiani, F., Klutsch, A., Jeffries, R. D., et al. 2017, A&A, 603, A81
de Bruijne, J. H. J., & Eilers, A.-C. 2012, A&A, 546, A61
de Vries, C. P. 1985, A&A, 150, L15
de Wit, W. J., Testi, L., Palla, F., & Zinnecker, H. 2005, A&A, 437, 247
Garrison, R. F., Hiltner, W. A., & Schild, R. E. 1977, ApJS, 35, 111
Gies, D. R., & Bolton, C. T. 1985, JRASC, 79, 233
Goy, G. 1973, A&AS, 12, 277
Grunhut, J. H., Wade, G. A., Sundqvist, J. O., et al. 2012, MNRAS, 426, 2208
Gull, T. R., & Sofia, S. 1979, ApJ, 230, 782
Gvaramadze, V. V., & Bomans, D. J. 2008, A&A, 490, 1071
Gvaramadze, V. V., & Gualandris, A. 2011, MNRAS, 410, 304
Harmanec, P., Holmgren, D. E., Wolf, M., et al. 2014, A&A, 563, A120
Hiltner, W. A., Garrison, R. F., & Schild, R. E. 1969, ApJ, 157, 313
Hoogerwerf, R., de Bruijne, J. H. J., & de Zeeuw, P. T. 2000, ApJ, 544, L133
Hoogerwerf, R., de Bruijne, J. H. J., & de Zeeuw, P. T. 2001, A&A, 365, 49
House, F., & Kilkenny, D. 1978, A&A, 67, 421
Kaper, L., van Loon, J. T., Augusteijn, T., et al. 1997, ApJ, 475, L37
Keenan, F. P., & Dufton, P. L. 1983, MNRAS, 205, 435
Kendall, T. R., Lennon, D. J., Brown, P. J. F., & Dufton, P. L. 1995, A&A, 298, 489
Kilkenny, D. 1974, Observatory, 94, 4
Kilkenny, D. 1993, South African Astronomical Observatory Circular, 15, 53
Kobulnicky, H. A., Chick, W. T., Schurhammer, D. P., et al. 2016, ApJS, 227, 18
Lau, H. H. B., Potter, A. T., & Tout, C. A. 2011, MNRAS, 415, 959
Lennon, D. J., Dufton, P. L., & Fitzsimmons, A. 1992, A&AS, 94, 569
Lennon, D. J., van der Marel, R. P., Ramos Lerate, M., O'Mullane, W., & Sahlmann, J. 2017, A&A, 603, A75
López-Santiago, J., Miceli, M., del Valle, M. V., et al. 2012, ApJ, 757, L6
Lutz, T. E., & Kelker, D. H. 1973, PASP, 85, 573
Maíz Apellániz, J. 2001, AJ, 121, 2737
Maíz Apellániz, J. 2004, PASP, 116, 859
Maíz Apellániz, J. 2005, in The Three-Dimensional Universe with Gaia, eds. C. Turon, K. S. O'Flaherty, & M. A. C. Perryman, ESA SP, 576, 179
Maíz Apellániz, J. 2013, Highlights of Spanish Astrophysics, 7, 657
Maíz Apellániz, J., Pérez, E., & Mas-Hesse, J. M. 2004a, AJ, 128, 1196
Maíz Apellániz, J., Walborn, N. R., Galué, H. Á., & Wei, L. H. 2004b, ApJS, 151, 103
Maíz Apellániz, J., Walborn, N. R., Morrell, N. I., Niemelä, V. S., & Nelan, E. P. 2007, ApJ, 660, 1480
Maíz Apellániz, J., Alfaro, E. J., & Sota, A. 2008, ArXiv e-prints [arXiv:0804.2553]
Maíz Apellániz, J., Sota, A., Walborn, N. R., et al. 2011, Highlights of Spanish Astrophysics, 6, 472
Maíz Apellániz, J., Pellerin, A., Barbá, R. H., et al. 2012, ASP Conf. Ser., 465, 484
Maíz Apellániz, J., Sota, A., Morrell, N. I., et al. 2013, in Massive Stars: From α to Ω, a Conference Held on 10–14 June 2013 in Rhodes, Greece, 198
Maíz Apellániz, J., Evans, C. J., Barbá, R. H., et al. 2014, A&A, 564, A63
Maíz Apellániz, J., Alfaro, E. J., Arias, J. I., et al. 2015a, Highlights of Spanish Astrophysics, 8, 603
Maíz Apellániz, J., Negueruela, I., Barbá, R. H., et al. 2015b, A&A, 579, A108
Maíz Apellániz, J., Sota, A., Arias, J. I., et al. 2016, ApJS, 224, 4
Maíz Apellániz, J., Alonso Moragón, A., Ortiz de Zárate Alcarazo, L., & The GOSSS Team 2017a, Highlights of Spanish Astrophysics, 9, 509
Maíz Apellániz, J., Barbá, R. H., Simón-Díaz, S., Negueruela, I., & Trigueros Páez E. 2017b, in The Lives and Death-Throes of Massive Stars, eds. J. J. Eldridge, J. C. Bray, L. A. S. McClelland, & L. Xiao, IAU Symp., 329, 140
Maíz Apellániz, J., Barbá, R. H., Simón-Díaz, S., et al. 2018, A&A, 615, A161
Malkov, O. Y., Oblak, E., Snegireva, E. A., & Torra, J. 2006, A&A, 446, 785
Martin, J. C. 2004, AJ, 128, 2474
Mason, B. D., Hartkopf, W. I., Gies, D. R., Henry, T. J., & Helsel, J. W. 2009, AJ, 137, 3358
McClintock, J. E., Rappaport, S., Joss, P. C., et al. 1976, ApJ, 206, L99
McEvoy, C. M., Dufton, P. L., Smoker, J. V., et al. 2017, ApJ, 842, 32
Mdzinarishvili, T. G. 2004, Astrophysics, 47, 155
Mdzinarishvili, T. G., & Chargeishvili, K. B. 2005, A&A, 431, L1
Meurs, E. J. A., Fennell, G., & Norci, L. 2005, ApJ, 624, 307
Michalik, D., Lindegren, L., & Hobbs, D. 2015, A&A, 574, A115

Miroshnichenko, A. S., Chentsov, E. L., & Klochkova, V. G. 2000, A&AS, 144, 379
Moffat, A. F. J., Marchenko, S. V., Seggewiss, W., et al. 1998, A&A, 331, 949
Moldón, J., Ribó, M., Paredes, J. M., et al. 2012, A&A, 543, A26
Morgan, W. W., Code, A. D., & Whitford, A. E. 1955, ApJS, 2, 41
Musaev, F. A., & Chentsov, E. L. 1989, Sov. Astron. Lett., 15, 360
Negueruela, I. 2004, Astron. Nachr., 325, 380
Noriega-Crespo, A., van Buren, D., & Dgani, R. 1997, AJ, 113, 780
Peri, C. S., Benaglia, P., & Isequilla, N. L. 2015, A&A, 578, A45
Popper, D. M. 1966, AJ, 71, 175
Poveda, A., Ruiz, J., & Allen, C. 1967, Boletin de los Observatorios Tonantzintla y Tacubaya, 4, 86
Ribó, M., Paredes, J. M., Romero, G. E., et al. 2002, A&A, 384, 954
Sayer, R. W., Nice, D. J., & Kaspi, V. M. 1996, ApJ, 461, 357
Schilbach, E., & Röser, S. 2008, A&A, 489, 105
Silva, M. D. V., & Napiwotzki, R. 2011, MNRAS, 411, 2596
Simón-Díaz, S., Caballero, J. A., Lorenzo, J., et al. 2015a, ApJ, 799, 169
Simón-Díaz, S., Negueruela, I., Maíz Apellániz, J., et al. 2015b, Highlights of Spanish Astrophysics, 8, 581
Simpson, R. J., Povich, M. S., Kendrew, S., et al. 2012, MNRAS, 424, 2442
Sota, A., Maíz Apellániz, J., Walborn, N. R., et al. 2011, ApJS, 193, 24
Sota, A., Maíz Apellániz, J., Morrell, N. I., et al. 2014, ApJS, 211, 10
Stone, R. C. 1978, AJ, 83, 393
Stone, R. C. 1982, ApJ, 261, 208
Stone, R. C. 1991, AJ, 102, 333
Sutantyo, W. 1975, A&A, 41, 47
Szczerba, R., Siódmiak, N., Stasińska, G., & Borkowski, J. 2007, A&A, 469, 799
Tetzlaff, N., Neuhäuser, R., Hohle, M. M., & Maciejewski, G. 2010, MNRAS, 402, 2369
Tetzlaff, N., Neuhäuser, R., & Hohle, M. M. 2011, MNRAS, 410, 190
Tokovinin, A., Mason, B. D., & Hartkopf, W. I. 2010, AJ, 139, 743
van Buren, D., & McCray, R. 1988, ApJ, 329, L93
van Buren, D., Noriega-Crespo, A., & Dgani, R. 1995, AJ, 110, 2914
van Leeuwen, F. 2007, Astrophys. Space Sci. Lib., 350, 20
Vijapurkar, J., & Drilling, J. S. 1993, ApJS, 89, 293
Walborn, N. R., Sota, A., Maíz Apellániz, J., et al. 2010, ApJ, 711, L143
Walborn, N. R., Sana, H., Simón-Díaz, S., et al. 2014, A&A, 564, A40
Walborn, N. R., Sana, H., Evans, C. J., et al. 2015, ApJ, 809, 109
Williams, S. J., Gies, D. R., Hillwig, T. C., McSwain, M. V., & Huang, W. 2013, AJ, 145, 29
Wisotzki, L., & Wendker, H. J. 1989, A&A, 221, 311
Wramdemark, S. 1980, A&AS, 41, 33